Biomechanical analysis of independent transfers: pilot study involving persons with paraplegia

by

Nethravathi Tharakeshwarappa

B.S. in Mechanical Engineering, Kuvempu University, India 1998

Submitted to the Graduate Faculty of

The School of Health and Rehabilitation Sciences in partial fulfillment

of the requirements for the degree of

Masters of Science in Rehabilitation Science and Technology

University of Pittsburgh

2005

UNIVERSITY OF PITTSBURGH

DEPARTMENT OF REHABILITATION SCIENCES AND TECHNOLOGY

This thesis was presented

by

Nethravathi Tharakeshwarappa

It was defended on

March 29, 2005

and approved by

Thesis Advisor: Alicia M. Koontz, Assistant Professor, Dept. of Rehabilitation Science and Technology, School of Health and Rehabilitation Sciences

---

Michael L. Boninger, Professor, Dept. of Physical Medicine and Rehabilitation, School of Medicine

---

Diane Collins, Assistant Professor, Dept. of Rehabilitation Science and Technology, School of Health and Rehabilitation Sciences

Biomechanical analysis of independent transfers: pilot study involving persons with paraplegia

Nethravathi Tharakeshwarappa

University of Pittsburgh

ABSTRACT

Transfers are crucial for independent mobility. However, transfers can cause problems if appropriate precautions are not considered. For instance, transfers can result in skin damage, overstretching of the low back, wrist and fingers, excessive motion in unstable spinal segments, and shoulder injury. The purpose of this study was to develop and evaluate a transfer measurement system, to determine an objective method to delineate the different phases of a transfer, and to determine the peak dynamic joint forces and moments at the wrist, elbow, and shoulder experienced by wheelchair users with paraplegia during a level tub bench transfer.

A transfer measurement system was developed which consists of a steel frame, two unistruts, two handrail attachments, two aluminum-mounting plates and two force-plates. A mock trial was conducted to determine whether the transfer systems performed correctly. The types of the transfer surfaces that we can evaluate include a tub bench, a toilet seat, and car seat. The phases of transfer from wheelchair to tub bench and back were identified based on force plate data and position and velocity of trunk marker (C7). The phase identification method was used to identify the approximate force coming on

the hand during tub bench transfer using force plate data. We studied nine paraplegic subjects transferring from wheelchair to level tub bench and back. We modeled the arm as a serial linkage mechanism in analyzing the peak dynamic joint forces and moments. It was found that peak net joint dynamic forces at the joints are greater in the trailing arm than in the leading arm. It was observed that the peak joint forces were minimum at the wrist and maximum at the shoulder in all nine subjects with paraplegia. The moments at the wrist were lower than the moments at the shoulder. In wheelchair to tub bench transfer, there was an inverse relationship between wrist force and transfer time. Examining leading and trailing arm forces in conjunction with transfer time may assist in modifying transfer styles in individuals with weakness, strength imbalance and shoulder pathologies.

Table of Contents

Table of Contents v

List of Figures ix

List of Tables xi

1 INTRODUCTION 1

1.1 Specific Aims And Hypothesis 2

1.2 Significance of Research 3

1.3 Thesis Organization 4

2 BACKGROUND 5

2.1 Types of independent transfers and surfaces 5

2.2 Upper extremity pain and transfers 6

2.3 Transfer related accidents 7

2.4 Biomechanical evaluations of transfers 8

Part I: Development of a Transfer System to Evaluate Kinetic And Kinematic Variables in the Selected Transfer Activities 12

3 METHODOLGY 12

3.1 Design, Fabrication and Securement of Transfer System 12

3.1.1 Tub bench 14

3.1.2 Toilet Seat 15

3.1.3 Car Seat 17

3.1.4 Trapeze 18

3.2 Instrumentation and Calibration 19

3.2.1 Load cell 19

3.2.2 Force-plates 23
3.2.3 Motion analysis system 23
3.2.4 Fast Track 25
3.3 Synchronization of data collected from all measurement systems 26
3.4 Initial arrangement of transfer system setup 27
3.5 Preliminary data from instruments during transfers 27
3.5.1 Car seat transfer 28
3.5.2 Tub bench transfer using trapeze 29
3.5.3 Tub bench transfer 29
3.5.4 Toilet seat transfer 29
3.6 Data Analysis 30
3.6.1 Load cell data 30
3.6.2 Kinematic data 30
3.6.3 Force plate data 31
3.6.4 Phase identification using force plate data and kinematic data 32
3.6.4.1 Leading and trailing arm forces 37
4 RESULTS 41
5 DISCUSSION 43
5.1 Transfer measurement system problems observed during transfers 43
5.2 Percentage of body weight transferred through the arm 45
Part II: Joint Forces During Lateral Transfers Among Persons with Paraplegia 48
6 METHODOLOGY 48
6.1 Subject Population 48

6.2 Kinematic Data collection 48
6.3 Data Analysis 50
6.3.1 Finding Joint Forces and Moments using Dynamic Force Analysis 51
6.3.1.1 Free body diagram of hand 56
6.3.1.2 Free body diagram of forearm 58
6.3.1.3 Free body diagram of upper arm 59
6.3.2 Transfer Time 60
6.3.3 Determining the Peak Forces and Moments at the Joints 61
6.3.4 Statistical Analysis 62
7 RESULTS 63
8 DISCUSSION 68
9 SUMMARY 73
APPENDIX A 76
APPENDIX B 82
APPENDIX D 86
APPENDIX E 88
APPENDIX F 92
APPENDIX G 96
APPENDIX H 99
APPENDIX I 102
APPENDIX J 105
APPENDIX K 107
APPENDIX L 110

APPENDIX M 113

APPENDIX N 116

APPENDIX O 119

APPENDIX P 122

APPENDIX Q 124

APPENDIX R 128

APPENDIX S 131

BIBLIOGRAPHY 137

List of Figures

Figure 1 Transfer System 13

Figure 2 Tube bench Brace 14

Figure 3 Peg 15

Figure 4 Bar 15

Figure 5 Tub bench secured using brace 15

Figure 6 Toilet seat secured using wood plate 16

Figure 7 Toilet seat setup with grab bar 16

Figure 8 : Mounting hardware for the load cell 17

Figure 9 Car seat and Grab bar setup 18

Figure 10 Frame for car seat 18

Figure 11 Trapeze setup 19

Figure 12. Schematic Diagram of load cell 21

Figure 13 Noise in load cell data (Zoomed view) 22

Figure 14 Force plate co-ordinate system 23

Figure 15 Camera co-ordinate system 24

Figure 16 Distance between Sensors 25

Figure 17 Time to transfer from wheelchair to tub bench using left force plate 31

Figure 18 Time to transfer from tub bench to wheelchair using right force plate 32

Figure 19 Right force-plate data 38

Figure 20 Left force-plate data 39

Figure 21 Cartesian coordinate of C7 39

Figure 22 Velocity components of C7 40

Figure 23 Improved overhead grab bar to minimize deflection 44

Figure 24 Horizontal grab bar with load cells installed on vertical wall 45

Figure 25 Illustration of experimental setup 49

Figure 26. Anatomical points for kinematic marker placement on the hand, wrist, and arm. 50

Figure 27 Schematic diagram of left arm with salient marker points 51

Figure 28 Free body diagram of Hand 56

Figure 29 Free body diagram of Forearm 58

Figure 30 Free body diagram of Forearm 59

Figure 31 Z-coordinate position of the C7 vertebral marker and different transfer phases 61

Figure 32 Peak wrist forces with transfer time during the wheelchair to the tub bench transfer (r = -0.69, p = 0.042). 66

Figure 33 Set position picture 106

Figure 34 Car Seat Transfer 112

Figure 35 Tub bench transfer using trapeze 115

Figure 36 Tub bench transfer without using trapeze 118

Figure 37 Toilet Seat Transfer 121

List of Tables

Table 1 Applied load (mean over 10 seconds) and positions used in the calibration of the load cell in Fz 21

Table 2 Noise in Fz (maximum peak to peak difference) at three locations for different load on grab bar 22

Table 3 Peak load cell forces 41

Table 4 Percentage of body weight measured by the load cell during transfers based on RF of load cell data 41

Table 5 Percentage of body weight transferred through the arm during a tub bench transfer 42

Table 6 Subject's demographic Information 48

Table 7 Peak resultant joint forces and moments during transfer from the wheelchair to the tub bench (leading arm) 63

Table 8 Peak resultant joint forces and moments during transfer from the tub bench to the wheelchair. (trailing arm) 64

Table 9 Paired sample test results for mean peak net joint dynamic forces values comparing transfer from wheelchair to tub bench and tub bench to wheelchair. Group means and standard deviations are in parentheses. 65

Table 10 Paired sample test results for mean peak net joint dynamic moment values comparing transfer from wheelchair to tub bench and tub bench to wheelchair. Group means and standard deviations are in parentheses. 65

Table 11 Pearson Correlation for peak joint forces with transfer time 66

Table 12 Pearson Correlation for peak joint moments with transfer time 67

Table 13. Time for Transfers to and from Tub Bench. Standard deviations are in parentheses. 67

Table 14 Comparison of the peak values during the loaded phase 69

Table 15 Comparison of the median values during lift phase 69

ACKNOWLEDGMENTS

I would like to thank my advisor, Dr. Alicia Koontz, for providing me with the leadership, opportunity, funding, and work environment to learn and conduct this research. I would also like to express my appreciation to Dr. Michael Boninger and Dr. Diane Collins for their insight, time, and guidance while serving as members of my thesis committee. I would like to thank other faculty, staff and students at the Human Engineering Research Lab. Additionally, I would like to thank everyone who helped directly or indirectly for the development of transfer measurement system and in the collection of the data for this study: Alexandra Jefferds, Megan Yarnall, Yushang Yang, Dr. Ding Dan, Erin Aghamehdi, John Duncan, and Bill Ammer .

I would also like to extend my deepest thanks to my parents and my In-laws for all the love, prayers, and support during these last few years here in Pittsburgh. Finally, I would like to thank my husband, William Roshan Quadros and my son Sathvik Jakins Quadros for all the love and support that they have provided, particularly over the last several months.

1 INTRODUCTION

The ability to transfer is extremely important for the functional independence of individuals with lower extremity dysfunction. Functional independence includes the ability to perform activities of daily living such as wheelchair propulsion, pressure relief, and transfers without the help of others. The upper extremity serves as the main means for independent transfers. Independent transfers are defined as the ability of an individual to fully move his or her self from a wheelchair to another surface or more generally, from one surface to another. The ability of individuals to transfer from a wheelchair independently is dependent on their upper extremity joint function and voluntary motor function(1;2). Eighty percent of individuals with a thoracic level SCI will be able to perform an independent transfer upon discharge from an inpatient stay at a rehabilitation facility(3). In a follow-up study of individuals with varying levels of SCI, 85% with paraplegia, 58% with incomplete tetraplegia and 16% with complete tetraplegia were able to perform chair transfers independently after three years post-discharge(4). Few studies have been published that describe transfer biomechanics in detail. In fact, one study by Nyland et al. recently disseminated a scientific review that summarized and identified the gaps in existing research on transfers(1). They state that comprehensive and accurate methods of describing transfer techniques are greatly needed and that "biomechanical modeling methods have not been used to estimate joint forces and moments during a transfer". They further stress that investigations on transfers are greatly needed to inform clinicians, physiatrists, and rehabilitation engineers who design assistive devices how to

better intervene with individuals with disabilities who strive to maintain the highest degree of independence.

The purpose of this study was to 1) develop a measurement system to evaluate transfer techniques, 2) determine an objective method to delineate the different phases of a transfer and 3) calculate the inverse dynamics of level wheelchair transfers for a group of persons with paraplegia.

The following specific aims and hypothesis were developed to accomplish this goal.

1.1 Specific Aims And Hypothesis

Specific Aim 1: Develop a measurement system for recording biomechanics of the upper limbs during selected transfer activities

A measurement system was needed to obtain a full depiction of the biomechanics of transfers. This required robust instrumentation to record upper limb forces/moments and body motion during various types of transfers. The system needed to be versatile to collect biomechanical measures for level as well as non-level surfaces and transfers that involve using some kind of support, for example, a grab bar, handle or trapeze.

Specific Aim 2: **Determine a method to objectively identify the phases of a transfer**.

A method was needed to objectively determine the timing of phases in order to isolate the moment of a transfer when the arms are bearing the weight of the body. This study examined a kinematic method based on 3D trunk movements.

Specific Aim 3: Determine the peak net wrist, elbow, and shoulder joint dynamic forces and moments for nine individuals with paraplegia during a level transfer from a wheelchair to tub bench.

Hypothesis 3a: Peak net joint dynamic forces and moments will be higher for persons who take less time to transfer.

Hypothesis 3b: Peak net joint forces and moments will be greater in the trailing arm than the leading arm.

1.2 Significance of Research

Previous studies have shown that individuals with SCI have a high prevalence of upper extremity (UE) repetitive strain injuries, such as shoulder impingement and carpal tunnel syndrome(1;5). Transfer activities, wheelchair propulsion, and pressure relief are the activities most closely associated with pain among individuals with SCI(1). Because these tasks allow interaction in the community and are associated with roles that are important for independence and self-care, it is important to determine accurate methods for describing transfer techniques in order to investigate the relationship between transfer technique and the development of pain and injury. This insight will aid in developing interventions targeted at reducing the prevalence of the upper extremity injuries among individuals with SCI improving comfort and quality of life as well as community integration. Because transfers have been associated with many wheelchair-related accidents, it is important to understand how individuals with lower extremity dysfunction transfer themselves from one surface to another and to identify techniques that minimize

the risk of falling and that preserve upper extremity function without causing extremely high forces and moments on the upper extremity joints.

1.3 Thesis Organization

The most important elements of this thesis were testing the transfer measurement system, determining the different phases of transfer, and calculating joint forces and moments using inverse dynamics.

The background section outlines the previous studies that were done on transfer studies, explains types of transfers, upper extremity pain and transfers, transfer-related accidents and biomechanical evaluations of transfers. The Methods section describes the development of transfer setup, the procedures and equipment used to collect data, the post-processing and data analysis procedure to obtain the final transfer variables and statistical analysis. The Results section outlines the findings of study. The Discussion section explains the findings and describes the implications. The Conclusion section describes limitations of the study, suggestions based on the findings in this study, and future work related to this study.

2 BACKGROUND

2.1 Types of independent transfers and surfaces

In general there are two types of independent transfers – even and uneven. An even transfer involves movement between two surfaces of equal heights. During an even transfer an individual brings his or her trunk forward, lifts the buttocks by pushing on the armrests, wheelchair seat, or wheel and while pivoting on the arms, swings the buttocks over to a level, adjacent surface. An uneven transfer involves a transfer to a lower or a higher surface. Uneven transfers are more difficult requiring greater skill and strength.

An individual may use a side, front or back approach to perform transfer activities. The side transfer is the most common type of transfer and works for a variety of even and uneven surfaces (e.g., from wheelchair to/from floor, vehicle, bed). The side approach is often preferred because it is fast and does not require a great deal of strength(2). The front approach doesn't require as much skill but it requires greater strength. The back approach is the most difficult requiring good shoulder flexibility, strength and fully innervated upper extremities(2). The choice in the approach used often depends on the space available where the transfer needs to occur. For example, bathrooms even those that are wheelchair accessible, do not offer much space for which to maneuver and position the wheelchair in the best position for the individual to transfer to the toilet seat.

To be independent in side, even transfers, without an assistive device an individual must be able to move, position and stabilize his/her trunk using the upper limbs. To accomplish

this often involves compensatory movement strategies such as muscle substitution, momentum, and the 'head-hips' relationship in which the individual pivots on his/her arms, moving the head downward and opposite to the direction of transfer in order to lift the buttocks(2). The 'head-hips' relationship is thought to be a compensatory movement strategy adopted by individuals with a greater level of impairment(6).

Since there is no scientific evidence available on the most appropriate way to transfer, clinicians have been faced with the challenge of using general ergonomic principles and clinical experience to determine the safest and most effective transfer method for their patients to use. Thus, Specific Aims 1, and 2 in this study focus on developing a transfer measurement system, determining whether the measurement system performs correctly during transfers and determining a method to objectively separate the phases of a transfer.

2.2 Upper extremity pain and transfers

Transfers along with pressure relief and wheelchair propulsion have been reported as the primary sources of upper extremity pain among individuals with SCI (7)(8;9). Dalyan et al. studied upper extremity pain reported by individuals with varying levels of SCI and the association with ten functional activities (7). Sixty five percent (36/55) of the individuals reported that pain interfered with transfer performance. Nichols et al. reported that 51.4% of 538 individuals with SCI experienced shoulder pain and 92% of these individuals noted wheelchair propulsion and transfers as primary reasons (8). Sie et al. studied the relationship between SCI and shoulder pain which was defined as significant pain that 1) required analgesic medication, 2) was associated with two or more

activities of daily living, or 3) was intense enough to warrant activity cessation. Thirty-two percent of the individuals had pain one-year following their SCI and 66% had symptoms of carpal tunnel syndrome(10). Curtis et al. reported that activities requiring high levels of upper extremity strength such as ascending a ramp in a wheelchair, overhead reaching, washing their backs, and transfers to non-level surfaces were most closely associated with intense shoulder pain (11).

It is apparent from the reported associations between upper extremity pain and transfer performance that developing transfer strategies that ameliorate upper extremity pain is desperately needed. A biomechanical analysis of transfer technique may provide insight into the potential causes of wrist and shoulder problems. Specific Aim 3 calculates the dynamic forces and moments for the wrist, elbow, and shoulder for a group of individuals with paraplegia during a level transfer.

2.3 Transfer related accidents

Transfers are responsible for many wheelchair-related accidents. Of the 770 wheelchair-related accidents leading to death that were reported to the U.S. Consumer Products Safety Commission between 1973 and 1987, 8.1% were caused by falls during transfers(12). Between 1986 and 1990, 16.9% of the estimated 36,559 wheelchair-related accidents that were serious enough to necessitate a visit to an emergency department were falls during transfers (13).

2.4 Biomechanical evaluations of transfers

Our review of the literature revealed only a few studies that looked specifically at the biomechanics of transfer activities. Allison et al. studied movement strategies during a side transfer of individuals with paraplegia and tetraplegia using force plates and a video camera that tracked markers attached to anatomical landmarks on the head, chest, arms and legs (6). They found that when viewed in the sagittal plane individuals used either a 'lift' or 'forward flexion' movement pattern and that the 'lift' technique was only used by individuals who had strong triceps. From a posterior view, two strategies could be discerned, 'translatory' and 'rotatory'. In the 'translatory' transfer, the head moves in concert with the iliac crest. In the 'rotatory' transfer, the head moves opposite of the iliac crest ('head-hips' relationship). All individuals who used the 'rotatory' transfer had weak triceps. The only kinetic measure reported in this study was the displacement of the center of pressure (COP) location which was not significant in predicting which transfer technique the individual used. A subsequent case study by Allison et al. investigated changes in the COP location during a side transfer with and without a custom trunk orthosis; however, there were also no significant differences in COP between the two conditions(14). One might question whether the experimental methods used in these two studies were not optimal for assessing side transfers. For the side transfer task, subjects used the same surface for the entire transfer (force plate) not two separate surfaces and subjects were not assessed in their ability to transfer from a wheelchair.

Studies that have addressed the electromyographic thoracohumeral muscle activation patterns during wheelchair transfer and weight-relief raise have shown different muscle

activation levels in different phases(9;15;16). Additionally, the patterns and relative magnitudes of glenohumeral and scapular muscle activation varied depending upon the upper extremity (leading or trailing arm) assessed during level transfer(16).

Improper wheelchair transfer may result in shoulder impingement that would escalate the pathology. Shoulder impingement syndrome has been reported to be the most commonly occurring pathology in the manual wheelchair population(17;18). Scapular upward rotation and posterior tipping elevate the anterior and lateral aspects of the acromion, the sites of shoulder impingement (19). Modest changes in scapular function lead to a reduction in this space, possibly increasing the potential for pathology(20). Alterations in scapular kinematics (increased internal rotation, reduced posterior tipping) and muscle activation patterns (increased upper and lower trapezius activity) have been reported to occur in individuals with shoulder impingement (21). To reduce the development of shoulder impingement, less injurious techniques should be investigated.

Finley et al., used telemetered electromyography to collect muscle activity and reported that scapular function during a leading limb and trailing limb transfer is different. They presented the differences among the transfers in peak EMG amplitude recorded throughout the complete range of each transfer. The trailing limb had increased serratus anterior and lower trapezius activity and reduced scapular upward rotation and posterior tip as compared with the lead limb transfer(18). They did not consider the effect of the magnitude of joint forces and moments in understanding the mechanism of shoulder impingement.

In an earlier study by Bayley et al. internal shoulder joint pressure measurements were performed on five pain-free shoulders of individuals with paraplegia who could independently transfer without the use of an assistive device (17). This was accomplished by inserting a sterile pressure-transducer under local anesthesia into the subacromial joint space. The results indicated that peak pressures during a transfer from the wheelchair to the bed were two and one-half times that recorded when the shoulder was in an unweighted position. The increased pressures appeared to be due to the shift in body weight from the trunk through the clavicle and scapula and across the subacromial tissues to the humeral head. The authors postulated that the high pressure in addition to the abnormal mechanical stress across the subacromial area during a transfer contributes to the high prevalence of shoulder problems among individuals with SCI.

Perry et al. conducted a fine-wire electromyographic analysis of the shoulder muscles during depression transfers in subjects with a T8 or below SCI(16). They separated the side transfer from the wheelchair to an adjacent examining table into three phases: preparation, lift and descent. The 'lift' phase required the greatest muscular effort by the lead arm with the pectoralis major muscle reaching approximately 81% of its' maximum voluntary contraction as determined by a manual muscle test. They suggested that the pectoralis major and latissimus dorsi muscles led to trunk elevation so long as the hand and humerus were stabilized. They postulated that these muscles, since they originate from the thorax and insert onto the humerus, help to circumvent glenohumeral joint compression during transfers and weight relief raises (15). Significant activity was also

noted for the serratus anterior which was needed to resist the upward rotation thrust on the scapula during weight-bearing. Rotator cuff muscles, infraspinatus and subscapularis, were most active during the lift phase and contributed to the laterally shifting of the trunk in the direction of the leading arm.

Wang et al. assessed uneven transfers of varying heights among six unimpaired subjects (22). Transfers to lower heights produced greater ground reaction forces and increased triceps brachii and posterior deltoid muscle effort to overcome gravity. Transfers to higher heights required greater biceps brachii muscle effort. Butler et al. conducted an accelerometric analysis of wheelchair-to-car transfers in unimpaired individuals(23). They determined that transferring the body in multiple stages versus in one movement was safer based on a reduction in area under the acceleration-time curve (velocity). In addition, there were no differences in body velocity when comparing feet-first transfers and body-first transfers.

While the above studies provide preliminary insight into side, even and uneven transfer techniques, nothing is known about transfers when some kind of assistive aid is used, such as a transfer board, handle, grab bar, or wheelchair arm rest. These aids are commonly used for transfers taking place from a wheelchair to a toilet, motor vehicle, or bed. This measurement system developed in this study is unique in that applied forces can be analyzed during transfers where a trapeze, a simulated handle or grab point in a motor vehicle (e.g., car transfer), and grab bar is used.

Part I: Development of a Transfer System to Evaluate Kinetic And Kinematic Variables in the Selected Transfer Activities

3 METHODOLGY

Developing the transfer system started with brainstorming design ideas with engineers, machinists and wheelchair users. Designs were clearly conveyed by using a CAD/CAM program to illustrate the system. The three dimensional models created on the CAD/CAM program ensured that the combination of parts would match correctly when assembled. Selection of machining methods was based on available resources at the Human Engineering Research Laboratories (HERL). Designs were revised as necessary during the machining stage based on these resources. All of the machining and welding were done at HERL. HERL has conventional milling machines and lathes along with computer numerically controlled (CNC) milling machines and lathes.

.

3.1 Design, Fabrication and Securement of Transfer System

The transfer system was developed to evaluate the kinetics and kinematics of the upper limbs when transferring from a wheelchair to a transfer surface. Types of transfer surfaces included a car seat, tub bench, tub bench with trapeze and toilet seat. Before construction of the transfer system, Solid works 2004 and Feature CAM were used to design the parts. Solid works 2004(Solid Works Corporation, Concord, Massachusetts) and Feature CAM (Engineering Geometry Systems Inc, Salt Lake City, UT) are computer aided design software. The transfer system consists of a steel frame, two unistruts, two

handrail attachments, two aluminum-mounting plates and two force-plates (see APPENDIX A). The frame are made of four inch steel channel, welded to create two three-foot square compartments (see Figure 1).

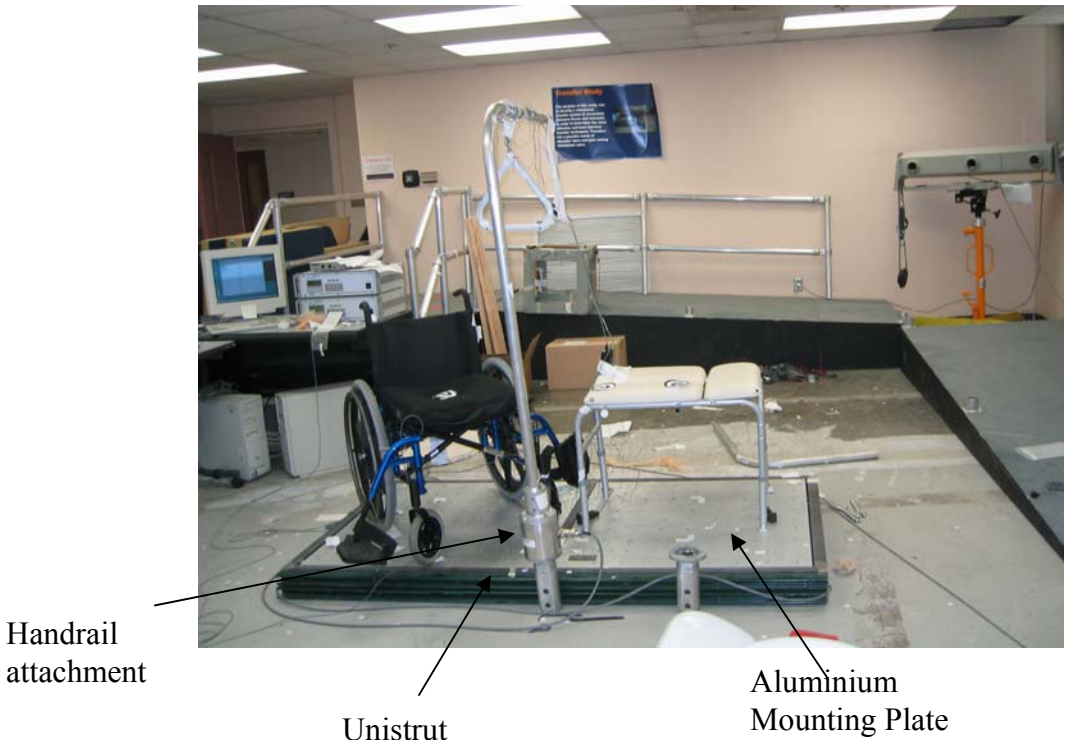

Figure 1 Transfer System

These square compartments housed the force-plates and aluminum mounting plates. The steel channel was cut using a power hacksaw and was MIG welded. The two unistruts were also cut using the power hacksaw and bolted to one side of the steel frame, providing an adjustable track for the handrail attachments to slide along. The mounting plate is three quarter inch aluminium plate. Threaded holes were drilled and tapped at equal intervals using a Jet manual mill.

3.1.1 Tub bench

In order for the tub bench to be rigid while easily variable for other setups, a way to lock and unlock the tub bench in place was necessary. The tub bench needed to be detached quickly and preferably without the need for tools. Figure 2 shows the tub bench brace which includes a peg and bar (see Figure 3 and Figure 4). Figure 5 shows how the tub bench attaches to the aluminium mounting plate using the brace.

Four pegs were cut using a power hacksaw. Quarter inch holes were horizontally drilled and tapped in the four pegs using a manual lathe. The Jet milling machine was used to drill and tap a quarter inch hole in the top center of the pegs. For the tub bench bar, a hole was drilled through one side and groove was made in the other side. This provided adjustability when bolting the brace to the aluminium plates.

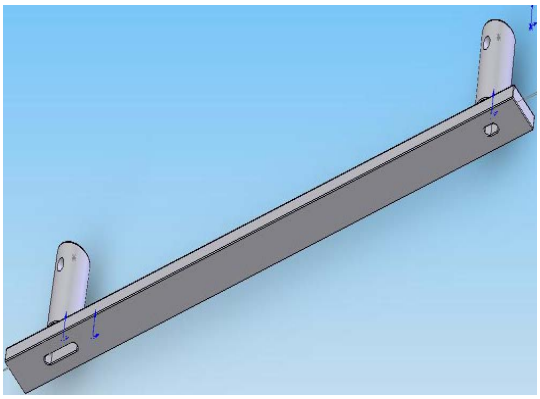

Figure 2 Tube bench Brace

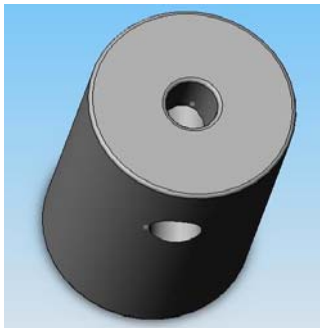

Figure 3 Peg

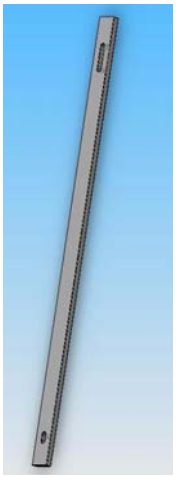

Figure 4 Bar

Figure 5 Tub bench secured using brace

The tub bench was secured to the force plate using the tub bench brace as shown in the Figure 5. The rubber bushes were removed from the ends of the tub bench legs, and the brace pegs were inserted into the legs. The tub bench is fastened to the tub bench brace using bolts and nuts. The tub bench was placed on the left mounting plate. The holes of the brace were aligned with those of the mounting plate and fastened down. The tub bench was leveled after being attached.

3.1.2 Toilet Seat

To secure a toilet to the mounting plate, an oval wooden base was made. The toilet was attached to the oval wooden base, which was then clamped to the left mounting plate as shown in Figure 6. The height of the toilet seat was increased by installing a one-piece molded raised toilet seat as shown in the Figure 6. The tapered flange of one-piece molded raised toilet seat fit directly on to the toilet bowl and provided a firm fit. For extra securement, we put tape in and around the elevated toilet seat.

Figure 6 Toilet seat secured using wood plate

Figure 7 Toilet seat setup with grab bar

According ADA (American disability act) side transfer (see APPENDIX B) a grab bar was positioned eighteen inches from the center of toilet seat towards the left as shown in Figure 7 . The grab bar was secured perpendicular to the front of the mounting plate using aluminum-mounting attachments. The grab bar attachments were composed of an AMTI MC5 series force/torque load cell(Advanced Mechanical Technology, Inc. Watertown, Massachusetts). The aluminum mounting attachments were composed of two separate pieces including a circular segment and a cylindrical piece. The circular segment was cut from a one-half inch aluminum sheet using a wire EDM (Electric Discharge Machining) machine. The solid aluminum cylinder was turned on a CNC Lathe. The two pieces were then MIG welded and eight through-holes were drilled around the circular face. One mounting attachment was screwed into the bottom of the load cell and was used to secure it to the unistrut. The second mounting attachment was screwed into the upper face of the load cell and supports the one and one half inch diameter aluminum handrail. The mounting hardware for the load cell is shown in Figure 8.

Figure 8 : Mounting hardware for the load cell

3.1.3 Car Seat

Figure 9 shows the car seat and overhead grab bar setup. As we wanted to simulate SUV (Sports utility vehicle) car seat transfer, measurement of SUV car (2000 Acura MDX) seat from floor was taken. The height of the car seat from ground was 75 cm. Therefore the frame was designed accordingly. A 3D- model of the frame was created in Solid Works software as shown in Figure 10. Then L-shaped channel was cut according to the dimensions as given in APPENDIX C.

The frame was attached to the car seat base using bolts and nuts. The car seat and frame were placed on the left force plate with the front right corner of the frame coinciding with the hole in mounting plate. The frame was then bolted down to the mounting plate rigidly to avoid displacement during motion transfer.

An overhead grab bar was made according to the height of an SUV car overheard grab handle(i.e 1.58m from the mounting plate). The overhead grab bar was cut and bent in the HERL machine shop. It was placed 1.58m from the platform to the grabbing position of the bar. The overhead grab bar was secured as explained above in section 3.1.2. The overhead grab bar was aligned perpendicular to the front of the mounting plate, above the right side of the car seat (see Figure 9).

Figure 9 Car seat and Grab bar setup

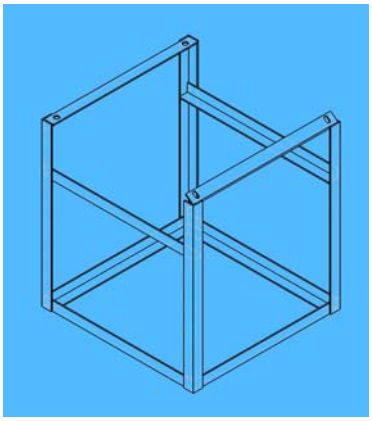

Figure 10 Frame for car seat

3.1.4 Trapeze

The trapeze is used by individuals with lower extremity dysfunction to change positions in bed and transfer from a bed to a chair with minimal assistance. In this study, the trapeze (Model 7941, Invacare Corporation, North Ridgeville, Ohio) was used to transfer from a wheelchair to a tub bench. We set the grab bar height to 1.55m and reach was set to 0.86m, which is used in Invacare fixed offset trapeze bar (24). This permitted use of the same over head grab bar that was used for the car transfer. The height of this grab bar was 1.58m and the reach height was set 0.86m from the surface of the mounting plate.

Trapeze was hung using a chain attached to the grab bar. The hook present at the end of the chain was inserted into the chain ring. For extra securement, chain of the Trapeze was tied to the grab bar using tape which is shown in the Figure 11.

Figure 11 Trapeze setup

3.2 Instrumentation and Calibration

3.2.1 Load cell

Calibration of many components of the transfer system was necessary in order to compare the recorded values to fixed, known values. The output of the amplifier from AMTI MC5 force/torque load cell was wired to a Connector Block (National Instruments). To record the forces and moments in horizontal, lateral and vertical

directions, we used a data acquisition card (DAQCard-6024E, 778269-01 National Instruments Corporation, Austin, TX) and Lab VIEW 6.1(National Instruments, Inc., Austin, TX). Figure 12 shows the schematic diagram of load cell. The AMTI MC5 force/torque load cell was calibrated by putting known weights at three positions A, B, and C and comparing the recorded values to actual known values. Known weights were added in the following increments: 4.55, 9.09, 13.64, 18.18, 22.73, 27.27, and 29.55 kg at each position. The data were recorded in volts from six channels including Fx, Fy, Fz, Mx, My and Mz. The maximum voltage for all channels was 5 volts. The data were then converted to kg and Newton using m-file *Loadcell.m* (see APPENDIX D). The recorded values at each position are given in Table 1.

We have observed the noise in load-cell voltage data as seen in Figure 13. The noise was measured as the difference between the maximum and minimum force (N) for a constant input weight. To identify the optimal location, i.e., location with minimum noise, we tabulated the noise at three locations for known weights (see Table 2).

Table 2 shows that low loads at position A gives more noise than Position B and C. At position C, channel My data were saturating for 22.73 Kg. At position A and B data of any channel were not saturated at 29.55 Kg. So to get good results, we chose the target position to grab the gab bar just before the position of B i.e 38.1cm from P.

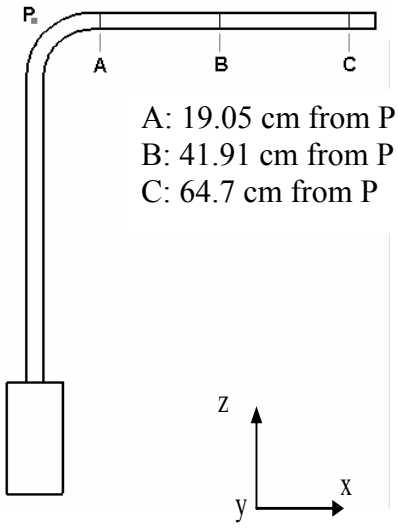

Figure 12. Schematic Diagram of load cell

Table 1 Applied load (mean over 10 seconds) and positions used in the calibration of the load cell in Fz

Trials	Actual Load(Kg)	Position A(Kg)	Position B(Kg)	Position C(Kg)
1	4.55	5.91	4.59	4.79
2	9.09	9.73	9.68	9.58
3	13.64	14.00	13.86	14.57
4	18.18	18.95	18.96	18.96
5	22.73	23.75	23.75	23.34
6	27.27	28.54	28.54	27.93
7	29.55	30.77	30.83	30.27

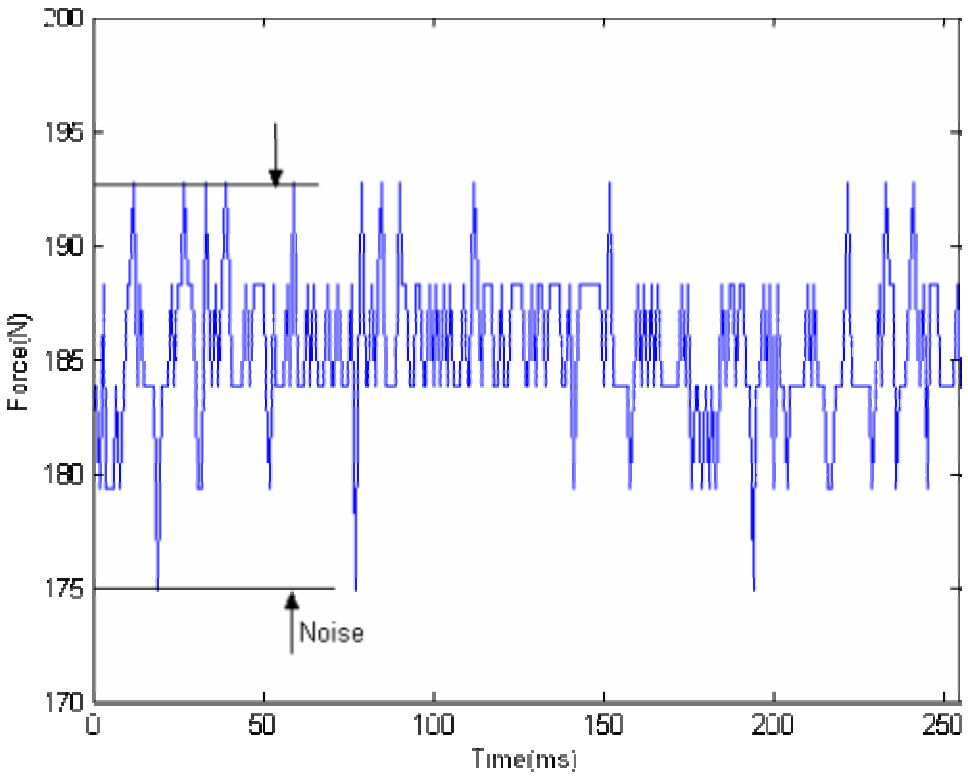

Figure 13 Noise in load cell data (Zoomed view)

Table 2 Noise in Fz (maximum peak to peak difference) at three locations for different load on grab bar

Trials	Actual Load(Kg)	Position A(kg)	Position B(kg)	Position C(kg)
1	4.55	20.39	2.55	2.24
2	9.09	20.39	2.75	1.83
3	13.64	2.55	2.55	2.24
4	18.18	2.34	2.34	2.65
5	22.73	2.55	1.83	2.55
6	27.27	1.33	1.33	1.83
7	29.55	1.33	1.33	1.83

3.2.2 Force-plates

The Bertec Force Plates (Bertec Corporation, Columbus, OH) were calibrated prior to shipment. However, the force plates were tested by placing a known weight on the force plates and comparing the recorded value to the corresponding known value. The force collection from the Bertec force plates involved the use of two amplifiers and connecting cables. The output from the amplifiers was wired to a National Instruments CB-68LP I/O Connector Block. A data acquisition card, DAQCard-6024E (Model 778269-01 National Instruments Corporation, Austin, TX), was linked to the Connector Block and used with National Instruments Lab VIEW 6.1 software to record the forces and moments in the x, y and z directions.

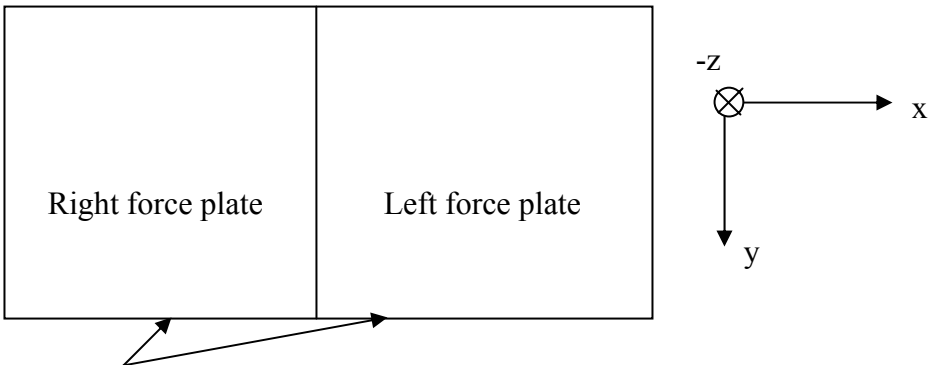

Figure 14 Force plate co-ordinate system

3.2.3 Motion analysis system

Two OPTOTRAK(Northern Digital Inc. Waterloo, Canada. Model 3020) real–time motion analysis systems were used in this study(25-28). Two OPTOTRAK camera cables were used to connect to the computer that collected the data. The markers connect to four six-way connectors that are joined together by cables. One Universal cable connects from

the six-way connectors to one of the two OPTOTRAK cameras. The markers were used to determine the x, y and z coordinates of the subject with respect to an established origin. The data collection system was then calibrated following a set procedure to establish the origin (see Figure 15). The origin was established at the back left corner of the steel frame and provided a relative location where accurate movement of the subject with respect to a specific point could be followed and analyzed (see APPENDIX E).

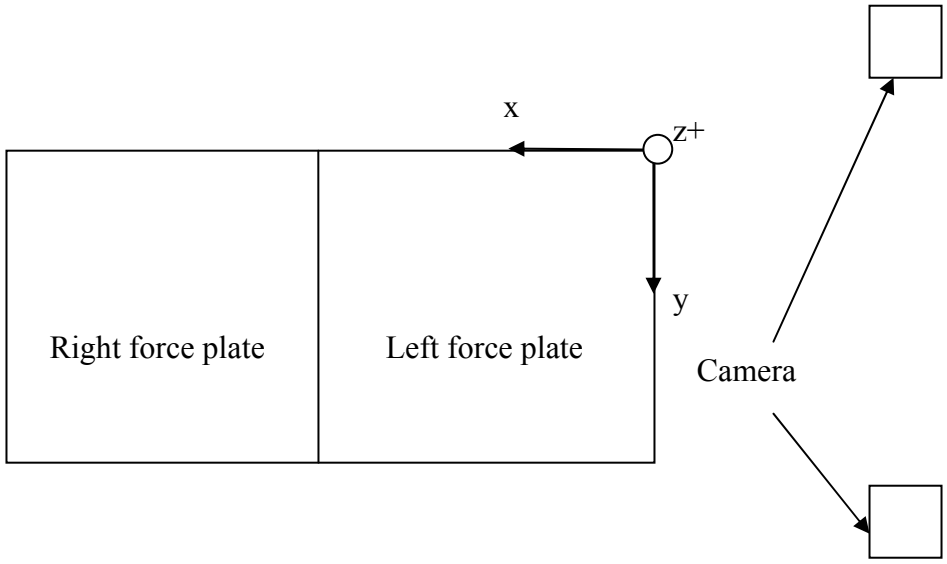

Figure 15 Camera co-ordinate system

3.2.4 Fast Track

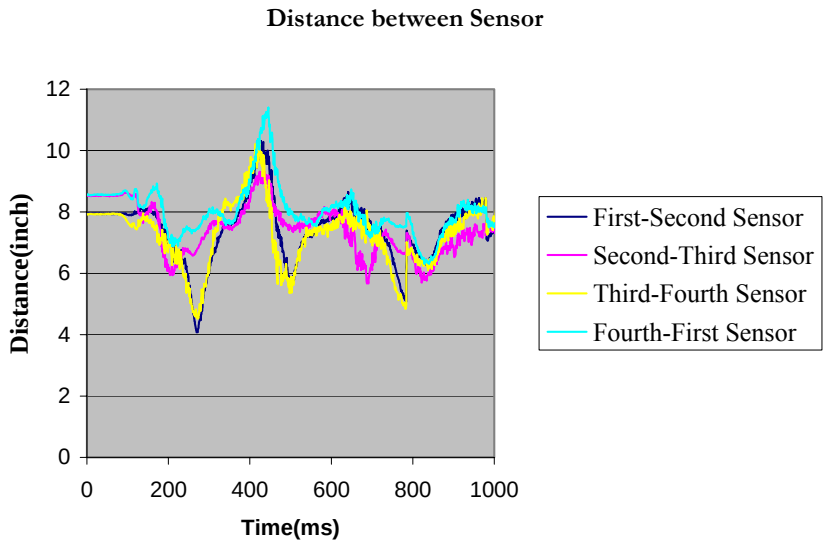

Figure 16 Distance between Sensors

We planned to use a FASTRAK (Pohlemus, Inc, Colchester, VT) electromagnetic system for the purposes of measuring upper limb motion during transfers. The benefit of an electromagnetic tracking system is that the sensors never get lost or become occluded because the human body as well as objects in the surrounding area are transparent to the electromagnetic waves. An additional benefit is that there is no digitizing or post-processing and the six-degree of freedom sensor provides x, y, z position and orientation (pitch, yaw, and roll).

For calibration purposes, we used a square box. Four FASTRAK sensors were placed 8 inches apart on the square box. The box was then moved around the transfer area and 10 sec data were collected for 3 trials. FASTRAK only reads in a semicircular position. Figure 16 shows the distance between each sensor while moving around the transfer area.

The first and third sensors showed a fairly accurate distance of 8 inches at the beginning. However, at 300 ms, the distance became 4 inches instead of 8 inches. That data collected from all four sensors were similarly unreliable so we decided not to use the FASTRAK electromagnetic system. The accuracy of the data may be affected by the presence of metal in the transfer system.

3.3 Synchronization of data collected from all measurement systems

The data synchronization system was developed to collect data from two force plates, two motion-analysis systems along with one load cell. The OPTOTRAK system generated a TTL(digital) signal that triggered the start of data collection from all other measurement systems. Data acquisition software had been developed for the force plates and load cells to accept trigger signal. The amplified-analog signals from the force plates and load cells were analyzed using customized Lab VIEW data-acquisition software (National Instruments, Inc., Austin, TX). A National Instruments data acquisition card (DAQCard-6024E) with analog-to-digital conversion capabilities was used in conjunction with Lab VIEW to read analog data from force plates and load cells. The data acquisition card features eight lines of digital input, sixteen lines of analog input, an amplifier, 12-bit analog to digital conversion, digital to analog conversation, and two lines of analog output. The general organization of the virtual instrument (VI) contains frame structure that includes two frames. The first frame is dedicated to scanning and displaying the data. The second frame performs the task of scanning the channels and writing the data to a file. A case structure controls which frame the program is in and how it arrives at that frame. The case structure includes three cases: continue the first frame, move it to the

second frame upon a mouse click command, and execute the first frame until a digital signal is received.

The VI was modified to read, process, and display from each force plate and load cell at a rate of 400 samples per second. In addition, the program had the option to collect for a specified period of time or to start collecting data on a mouse click signal or a digital TTL trigger signal.

3.4 Initial arrangement of transfer system setup

Transfer system included choice of four target surfaces such as tub bench, tub bench with trapeze, car seat, and toilet seat and one common wheelchair. Calibrated load cell along with calibrated OPTOTRAK cameras, and force-plates were connected to data collection computers. The OPTOTRAK signal was set to trigger the force-plates and load-cell to record data simultaneously. To record the baseline data, the force-plates and load-cell were zeroed before placing the wheelchair on the right side of the mounting plate (see Figure 14). To keep the wheelchair in stable position the wheel locks were activated. The right mounting plate data were recorded, which measures the wheelchair weight. Further details of four transfer system setup are discussed in the next section.

3.5 Preliminary data from instruments during transfers

To evaluate the transfer measurement system and to develop a protocol for future studies, preliminary data from the instruments were collected while a design engineer on the

project performed to-and-fro transfers in four different transfer setups. Protocols were developed that can be used in the future studies to transfers for four test setups.

Markers were placed on the design engineer, wheelchair, and transfer surfaces (see APPENDIX F, APPENDIX G, APPENDIX H, and APPENDIX I), and before collecting the data from the instruments, cameras were adjusted until all markers were visible. Then the data were visualized using Matlab (MathWorks Inc.) program file *Movie.m* (see APPENDIX K) to make sure that the all markers were visible. If some of the markers were missing, then cameras were adjusted. This process was repeated until all markers were visualized using Matlab program.

3.5.1 Car seat transfer

The car seat was secured to the left side of the mounting plate. The load-cell was positioned between the car seat and wheelchair to simulate a transfer from a SUV to wheelchair and back again. An overhead grab-bar was attached to the load-cell. Baseline data of the force plate and load cell were recorded. The OPTOTRAK camera markers were placed on the anatomical landmarks, wheelchair, car seat, and overhead grab bar (see APPENDIX G). Design engineer tried not to use legs, tried not to put weight on legs, and tried to keep legs on the mounting plate while transferring. A protocol was developed to evaluate a car seat transfer in a future study (see APPENDIX L).

3.5.2 Tub bench transfer using trapeze

The tub bench was set level with the wheelchair as shown in APPENDIX M. The wheelchair was retained at 45 degrees to the tub bench. The OPTOTRAK camera markers were placed (see APPENDIX H). Target points were marked with black and white colored circles to give a clear idea to the design engineer where to place hands and bottoms while transferring to tub bench. Design engineer tried not to use legs, tried not to put weight on legs, and tried to keep legs on the mounting plate, while transferring from the wheelchair to the tub bench and back in about twenty seconds. A protocol was developed to evaluate a tub bench transfer using trapeze in a future study (see APPENDIX M).

3.5.3 Tub bench transfer

Using the same set up (as described in Section 3.5.2) but without the trapeze, the design engineer transferred from the wheelchair to the tub bench and back. A protocol was developed to evaluate a tub bench transfer in a future study (see APPENDIX N).

3.5.4 Toilet seat transfer

The tub bench was replaced with the toilet seat. The overhead grab-bar was removed and the load-cell was moved to the left side of the toilet seat. The grab-bar was set 18 inches from the center of the grab-bar towards the toilet seat as per ADA (American Disability Act). The wheelchair was secured at a 30 degree angle with respect to the toilet seat. OPTOTRAK camera markers were placed (see APPENDIX I). Target points were marked with black and white colored circles to give a clear idea to design engineer where

to place their hands and bottoms while transferring to toilet seat. Based on the observations made in transferring from wheelchair to toilet seat and back, a protocol was developed for future studies (see APPENDIX O).

3.6 Data Analysis

After the data collection, data were post-processed using several conversion programs in Matlab (MathWorks, Inc.) All raw data were filtered using 4th order Butterworth digital filter the signal, with a cutoff frequency of 20/200 Hz (where 200 = half of force plate and load cell sampling rate) to smooth each individual signal.

3.6.1 Load cell data

Raw voltage data were collected for all trials from load cell at a sampling frequency of 400 Hz. Voltage data were converted to forces (Newton) and moments (Nmm) using the m-file *Loadcell.m* (see APPENDIX D). Using these force components, resultant force was calculated. Then peak force while transferring from wheelchair to target surfaces and back was recognized using the m-file *Twopeakloadcell.m.* (see APPENDIX P)

3.6.2 Kinematic data

Raw kinematic data were collected at a sampling frequency of 60 Hz. Raw kinematic data for each marker were converted into three-dimensional distances (mm) from a global co-ordinate system origin according to previous calibration in OPTOTRAK. Due to occasional marker obstruction from camera view during transfer trials, all files were checked for missing data points and cleaned if necessary by a smoothing function created

in the interpolation m-file (see APPENDIX Q). This program interpolated between and replaced any missing points.

3.6.3 Force plate data

Raw voltage data were collected for all trials by force plate at a sampling frequency of 400 Hz. Force plate data collected were in voltages. Data collected during the tub bench transfer were converted from voltage data to forces (Newton) and moments (Nmm) using the m-file *Forceplate.m* (see APPENDIX R). A method was devised to determine transfer time using force plate data. The point where force starts increasing was taken as start time and end time was taken when the force stabilizes as shown in Figure 17 and Figure 18.

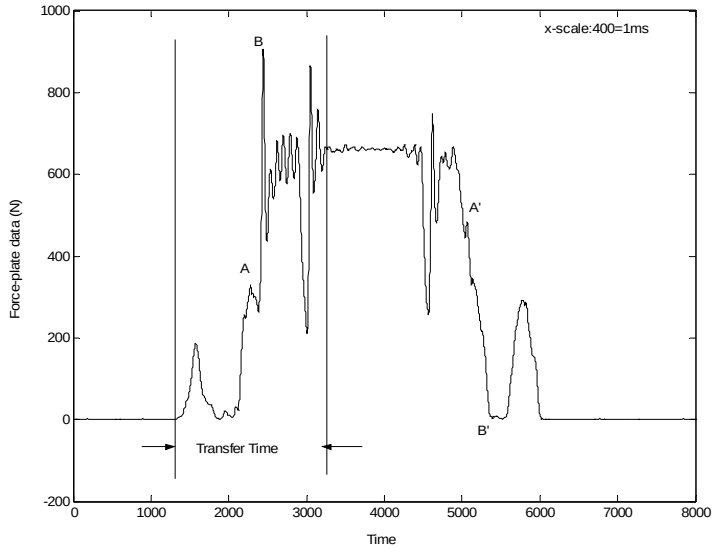

Figure 17 Time to transfer from wheelchair to tub bench using left force plate

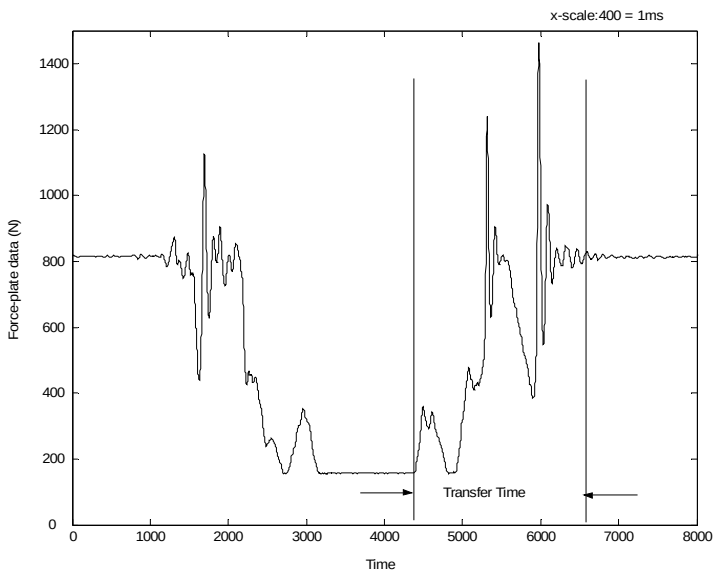

Figure 18 Time to transfer from tub bench to wheelchair using right force plate

3.6.4 Phase identification using force plate data and kinematic data

The force plate data and position and velocity of C7 were used to identify the different phases during tub bench transfer. A slight slide was experienced during transfers when the hand was pressed against the tub bench and wheelchair. Hence, no consistent characteristics were observed in Fx and Fy. Fx and Fy components were much lower than Fz. Therefore, phases were identified based on vertical component, Fz. Here the movement of C7 in horizontal plane was observed for identifying the phases. Therefore, the position and velocity of X and Y coordinates of C7 were used in identifying the phases. An example consisting of nine phases of tub bench transfer is shown in Figure 19 to Figure 22. In the following paragraphs, the details of the phases are described.

Phase I: Stationary phase in wheelchair

The right plate reads the weight of the design engineer and wheelchair, which is about 821.2 N as seen in Figure 19. The left plate data stays at zero as seen in Figure 20 as the design engineer's weight is entirely on the right plate. The X and Y coordinate of C7 remains constant (1826mm in X-coordinate and 1260mm in Y-coordinate) and hence the velocity, which is the first derivative of position, remains at zero (see Figure 21 and Figure 22).

Phase II: Preparation phase for wheelchair to tub bench transfer

In this phase, the design engineer places her leading (left) hand on the tub bench (at a near-target location) and scoots forward by moving the bottom to the front-left corner of the wheelchair seat. As the design engineer presses against the tub bench, an increase in the left force plate reading is seen in Figure 20. As the force reading increases in the left plate, the reading in the right plate decreases. At this point the bottom is above the wheelchair seat. At next instance design engineer places her bottom at the corner of the wheelchair seat. This can be observed in Figure 19 by noticing a sharp increase in the right-plate reading. Due to the impact load, the right force plate reads more than initial reading of 821.2 N and reaches about 1112 N as seen in Figure 19. At the time of impact, X-coordinate reaches the local minimum of this phase, i.e., the design engineer is in the extreme left position of this phase. Similarly, the Y-coordinate reaches local maximum of this phase, i.e., the design engineer is in the extreme front position of this phase. At the end of this phase the design engineer moves settles at the front-left corner of the

wheelchair, which can be seen by a increase in the X-coordinate and slight decrease in the Y-coordinate of C7.

Phase III: Transfer phase from wheelchair to tub bench

In this phase, the design engineer moves from wheelchair to tub bench completely. As the design engineer moves, the force in her leading (left) arm increases until point A^1 (330.1 N), as shown in Figure 20. Consequently, the right force-plate reading decreases until point A (451.8N), which is a measure of force in the trailing (right) arm (see Figure 19). At this point, the bottom is located above the tub bench. Design engineer's bottom lands on the tub bench, which is identified by a sharp increase in the left force-plate reading (see point B^1 in Figure 20) and sharp decrease in the right force-plate reading (see point B in Figure 19). By the end of this transfer phase, the right force-plate reading goes to the global minimum, i.e., the right force-plate reads only the dead weight of the wheelchair. Note that in this phase X-coordinate of C7 decreases (see Figure 21), i.e., design engineer moves towards the left onto the tub bench. Variation in Y-coordinate of C7 is minimal as the wheelchair and tub bench were aligned (see Figure 21)(see Camera coordinate system in Figure 15).

Phase IV: Repositioning phase on tub bench

In this phase, the design engineer repositions on the tub bench by moving towards the center of the tub bench. As the design engineer repositions, a spike in the right force plate is seen in Figure 19 because her pushes the wheelchair while repositioning using her trailing (right) arm. At this instance, a sharp decrease in left force plate data is observed

in Figure 20 as the bottom lifts up while repositioning. In the next instance, the bottom lands back on the tub bench, which results in a sharp increase in left force plate reading (866N), due to impact, as seen in Figure 20. At the end of this phase, right force plate reading goes to a minimum and left force plate reads a steady value. The X-coordinate of C7 decreases and stays at a minimum point, i.e., body moves left towards the center of the tub bench. No large change in Y-coordinate is seen as the design engineer moves almost parallel to X-axis.

Phase V: Stationary phase in tub bench

In this phase, the design engineer stays in set position on the tub bench. The position of C7 remains constant; hence velocity of C7 stays at zero as seen in Figure 22. Both the force plates read constant force (see Figure 19 and Figure 20).

Phase VI: Preparation phase for tub bench to wheelchair transfer

In this phase, the design engineer prepares for transfer by moving the body towards the wheelchair and by moving the bottom to the right corner of the tub bench. During the preparation phase, the design engineer exerts force on the wheelchair by placing her leading (right) arm on the wheelchair. This can be seen by observing a spike in the right force plate reading (see Figure 19). As the design engineer exerts force on the wheelchair, the bottom lifts up and a sharp decrease in the left force plate reading is observed (see Figure 20). In the next instance the design engineer places her bottom at the right corner of the tub bench and due to impact loading a sharp increase in the left

force plate reading is observed (see Figure 19). The X-coordinate of C7 increases at the end of this phase, i.e., the body moves towards the right (see Camera coordinate system in Figure 15). Also, the Y-coordinate of C7 increases slightly, indicating that the design engineer moved towards front.

Phase VII: Transfer phase from tub bench to wheelchair

In this phase, the design engineer places her leading (right) arm on the wheelchair and moves from the tub bench to the wheelchair. The force on the right force plate increases up to C (469.6N in Figure 19). Consequently, the force on the left force plate decreases to C^1 (474.6N in Figure 19) which is a measure of force in the trailing (left) arm. In the next instance the design engineer places the bottom on the wheelchair and a sharp increase in the right force plate reading is observed (see point D in Figure 19). At the end of this phase, the right force plate reading reaches 821.2N as observed in Phase I. The left force plate reading goes to zero as the design engineer completely moves from the tub bench to the wheelchair. At this point the design engineer is at the left corner of the wheelchair and the X-coordinate of C7 is 1680mm, which is slightly less than the initial position 1826mm (see Phase I).

Phase VIII: Repositioning phase in wheelchair

In this phase, the design engineer moves from the front-left corner of the wheelchair to the center of the wheelchair. As the design engineer repositions, a spike in the left force plate is seen because he pushes against the tub bench using her trailing (left) arm. At this instance, the reading in the right force plate decreases (see Figure 19 and Figure 20). In

the next instance, the bottom of the design engineer is positioned at the center of the wheelchair, this can be observed by a sharp increase in the right force plate reading due to impact. The right force plate reading stabilizes and at the end of this phase reaches 821.2N, which is the same as the weight of wheelchair and design engineer as seen in Phase I. Also, Figure 21 shows that X coordinates of C7 moves from 1680mm to 1826mm, i.e., she moves slightly towards her right.

Phase IX: Stationary phase in wheelchair

In all four graphs, the characteristics in Phase IX and Phase I are the same.

3.6.4.1 Leading and trailing arm forces

Using phase identification, the approximate force exerted on the hands during tub bench transfer can be ascertained. During wheelchair to tub bench transfer, maximum force in the leading arm (left) was 330.1N and trailing (right) arm calculated as 294.84N i.e 451.8N subtracted from 158N, where 158N is the wheelchair weight (See A in Phase III of Figure 19 and Figure 20) .

During tub bench to wheelchair transfer, maximum force in the trailing arm (left) was 474.6N and the leading (right) arm calculated as 311.6N i.e 469.6N subtracted from 158N, where 158N is the wheelchair weight (See C in Phase VII of Figure 19 and Figure 20) .

Percentage of body weight transferred through the leading arm was 54.83 % and trailing arm was 48.97% during wheelchair to tub bench. Percentage of body weight transferred through the leading arm was 51.76 % and trailing arm was 78.84% during tub bench to wheelchair transfer.

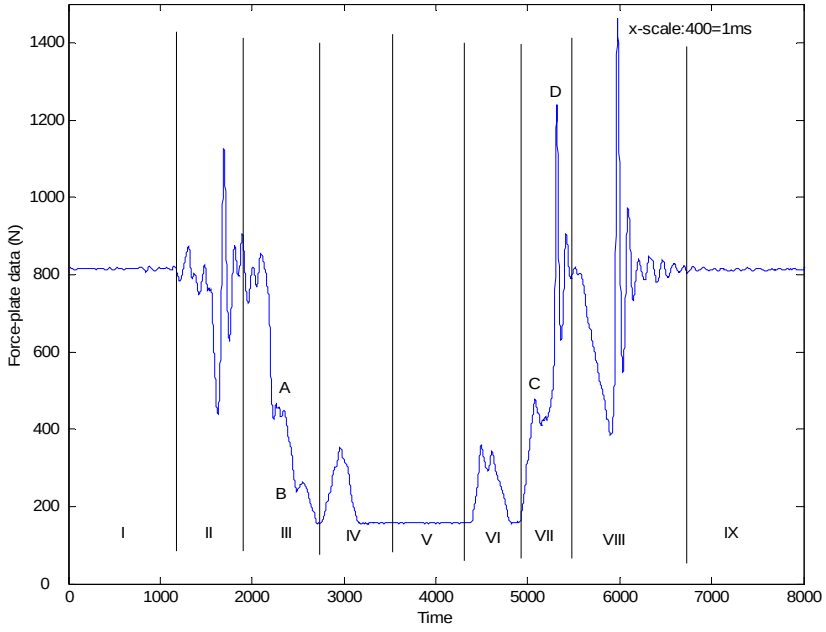

Figure 19 Right force-plate data

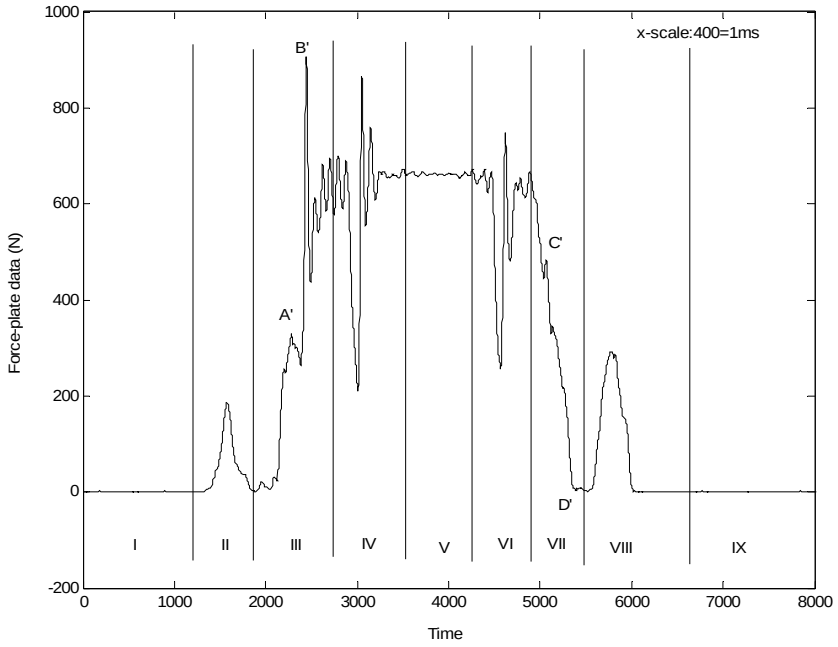

Figure 20 Left force-plate data

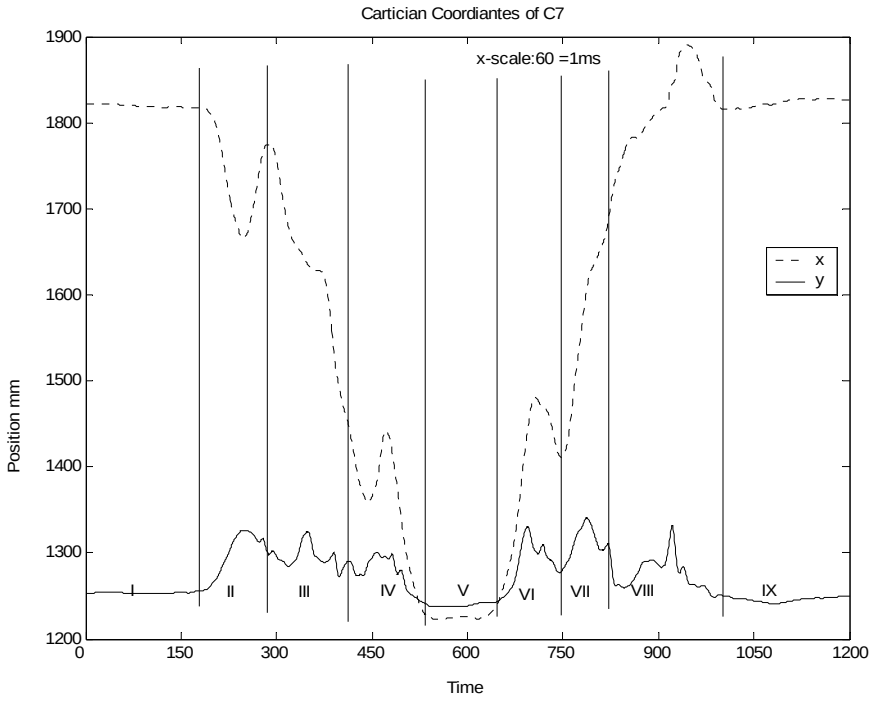

Figure 21 Cartesian coordinate of C7

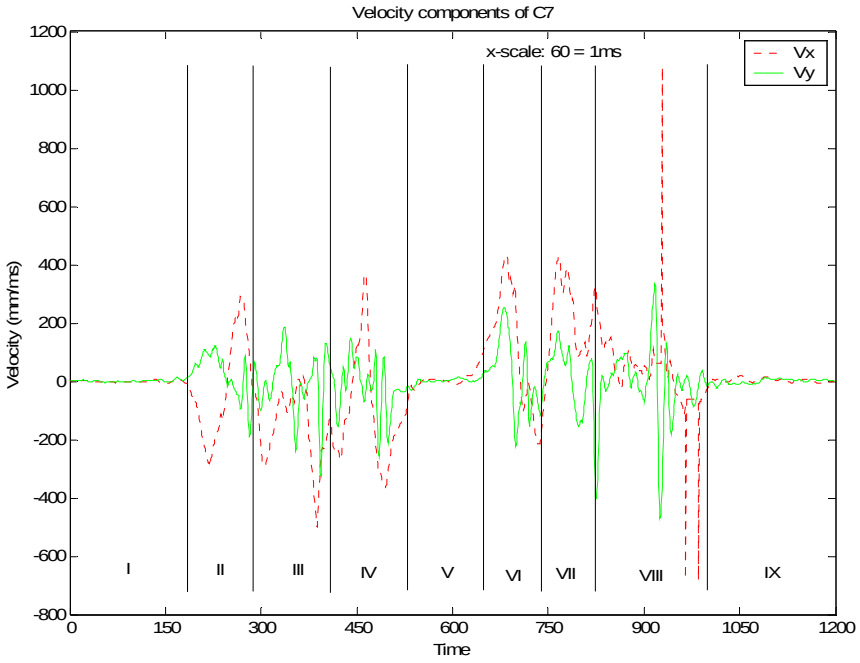

Figure 22 Velocity components of C7

4 RESULTS

Using the method described in Section 3.6.3, the transfer from the wheelchair to the tub bench was 1950ms and transfer from the tub bench to the wheelchair was 2250ms.

Table 3 Peak load cell forces

Peak Force	Fx	Fy	Fz	RF
Wheelchair to Car seat (leading(right) arm)	67.38	36.02	235.19	247.33
Car seat to Wheelchair (trailing(right) arm)	64.03	34.87	222.32	233.97
Wheelchair to tub bench with Trapeze (trailing(right) arm)	64.06	24.02	277.74	286.06
Tub bench with trapeze to Wheelchair (trailing(left) arm)	47.54	10.53	206.33	212.00
Wheelchait to toilet transfer (leading arm(left))	39.41	47.84	151.46	163.65
Toilet to wheelchair transfer (trailing arm(left))	40.48	57.56	146.88	162.87

Fx:anterior-posterior force, Fy:medial-lateral force, Fz:superior force, RF:Resultant force

Table 3 shows the peak load cell force components during transfer from wheelchair to target surfaces and back. Target surfaces are car seat, tub bench with trapeze and toilet seat.

Table 4 Percentage of body weight measured by the load cell during transfers based on RF of load cell data

Transfer	Percentage of body weight
Wheelchair to Car seat(leading(left) arm)	41.09
Car seat to Wheelchair(trailing(left) arm)	38.87
Wheelchair to tub bench with Trapeze(trailing(right) arm)	47.52
Tub bench with trapeze to Wheelchair(trailing(left) arm)	35.22
Wheelchait to toilet transfer(leading arm(left))	27.19
Toilet to wheelchair transfer(trailing arm(left))	27.06

Table 5 Percentage of body weight transferred through the arm during a tub bench transfer

Transfer	Percentage of body weight
Wheelchair to tub bench(leading(left) arm)	54.84
Tub bench to Wheelchair(leading(right) arm)	51.77
Wheelchair to tub bench(trailing(right) arm)	48.97
Tub bench to Wheelchair(trailing(left) arm)	78.84

5 DISCUSSION

This study was undertaken to evaluate the transfer system during transfers from wheelchair to target surfaces. Some of the problems and limitations associated with transfer measurement system method are discussed here. This section also proposes the possible improvements to alleviate problems in the current transfer measurement system.

5.1 Transfer measurement system problems observed during transfers

The observations made in transfers from wheelchair to four target surfaces are discussed in the following paragraphs.

During the transfer, it is observed that the wheelchair moved slightly. To avoid the movement of the wheelchair just applying the brakes was not enough. In the future, in order to collect reliable data, the wheelchair needs to be firmly fixed to the mounting plate. Therefore the wheelchair should be fastened down to the mounting plate with clamps.

During car seat transfer, slight deflection of the overhead grab bar was observed. In order to avoid the slight deflection during transfer, an additional truss/structural members needs to be welded/fastened between the two orthogonal tubes of 'L' shape cantilever (grab bar) to avoid the bending in vertical plane. One possible configuration to minimize the deflection is shown in Figure 23.

In tub bench with trapeze transfer, the trapeze attached to the overhead grab bar made the cantilever setup more unstable. Reliability of the data may be affected by the trapeze attachment. However, we needed to consider simulating the reality of the trapeze use in daily living of wheelchair users with spinal cord injury. Further investigation is needed to examine reliability with current setup.

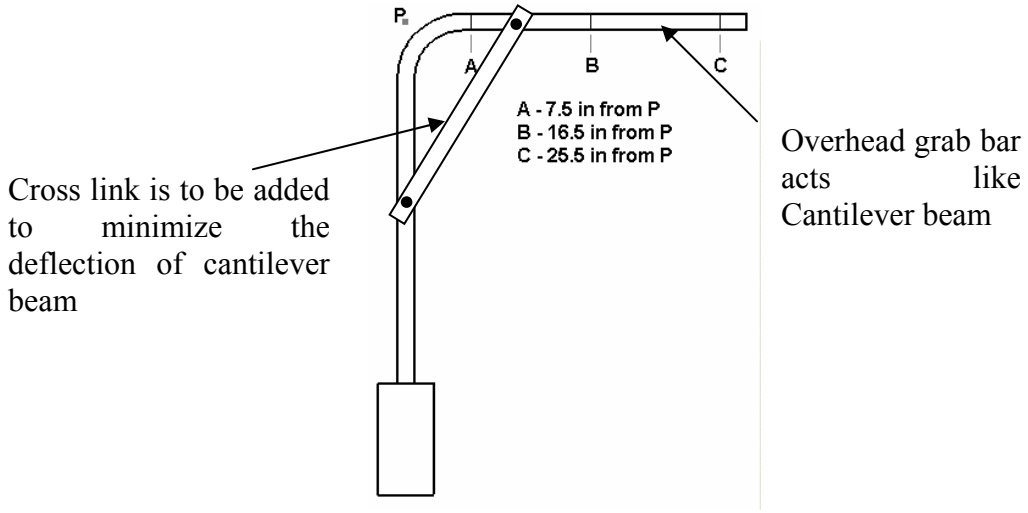

Figure 23 Improved overhead grab bar to minimize deflection

In toilet seat setup, the current experimental setup has a side grab bar whose fastener needs to be improved. The design engineer pushed/pulled the grab bar along the horizontal whereas in the other transfers, the design engineer leaned more vertically into or pulled down on the bar or trapeze. After the mock trial, handrail attachment to the grab bar had loosened. The instability of the attachment may attribute to the poor reliability of the load cell forces. To avoid the side deflection of the grab bar, the grab bar can be mounted on a vertical wall as shown in Figure 24.

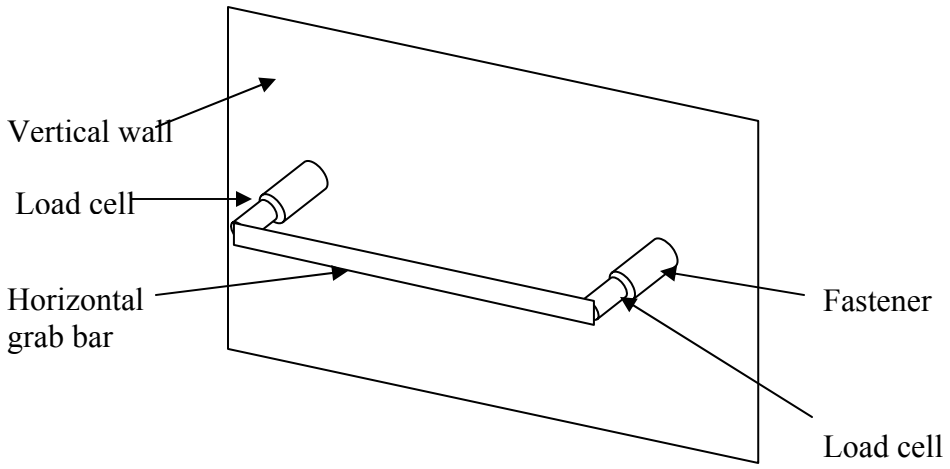

Figure 24 Horizontal grab bar with load cells installed on vertical wall

5.2 Percentage of body weight transferred through the arm

Forces in the arms during transfer phase in all four transfers were measured as a percentage of body weight. The potential causes for the changes in the forces in the to and fro transfers are highlighted. These forces in the hands are compared with previous results (available only for tub bench transfer) in measuring the effectiveness of the transfer measurement system.

In tub bench transfer, trailing arm forces were higher than leading arm, which matches with the result reported using EMG data by Perry et. al. (16). In this study, during wheelchair to tub bench transfer percentage of body weight transferred through the leading arm was 54.83%. Whereas, the percentage of body weight transferred through trailing arm was 78.84% during tub bench to wheelchair transfer. This could be because the trailing arm must support more weight as the design engineer pivots about the trailing

arm while transferring from the tub bench to the wheelchair. Also, other factors such as the added challenge of maneuvering back into the wheelchair, and the test setup position might have influenced the applied force measurement.

In car seat transfer, that is an uneven transfer, the leading arm force was 41.09 % of body weight during wheelchair to car seat transfer which is 2.22% more than the force in the trailing arm during car seat to wheelchair transfer. This could be because uneven transfer (i.e., car seat height was more than that of wheelchair) and design engineer movement against the gravity. While transferring from car seat to wheelchair, design engineer moved towards gravity, thus less force was experienced in the trailing arm. Further study in analyzing the force plate data might give more insight to know the forces exerted by both trailing arm and the leading arm during wheelchair to car seat and the car seat to wheelchair transfers.

In the tub bench transfers without the trapeze, the forces in the trailing arms were higher than the forces in the arms during tub bench transfer using trapeze. In the tub bench transfer using a trapeze, 47.52% and 35.22% of body weight were transferred in the trailing arm during wheelchair to tub bench transfer and tub bench to wheelchair transfer, respectively.

In toilet seat transfer, percentage of body weight transferred through the leading and trailing arms were the minimum on the load cell when compared to all the other transfers. This could be because during the transfer the arm was positioned along the transfer direction (left to right or right to left). Therefore, almost the whole weight of the body

does not come on a single arm, where as in other transfers a single arm has to support almost the whole body weight. Further study in analyzing the force plate data might give more insight to know the forces in the other arm during transfers.

From Table 3, it was observed that the influence of peak superior force on peak resultant force is more than other two force components (Fx and Fy). The peak anterior-posterior force (Fx) and peak medial-lateral force (Fy) were much less than peak superior force. This seems reasonable, because the design engineer seemed to use more forces applied in vertical direction (along z-axis) during transfers.

In the future, the methods that could be employed to perform more rigorous testing of the measurement system are briefly discussed below. Data can be collected from several unimpaired users. Also, instead of one trial, multiple trials can be taken. These data can then be analyzed to test the reliability/consistency of the measurement system and the protocol. This will also provide insight for calculating the minimum number of trials that is sufficient to obtain reliable data of the SCI (spinal cord injury) subjects using the Spear-Brown prediction formula(29).

Part II: Joint Forces During Lateral Transfers Among Persons with Paraplegia

6 METHODOLOGY

6.1 Subject Population

Nine manual wheelchair users with a spinal cord injury ranging from T4-L4 provided informed consent prior to participation in this study. Their average age was 44.1±12.3 years and their mean number of years since injury was 11.4±8.9. Table 6 shows the subject characteristics.

Table 6 Subject's demographic Information

Subject	Sex	Age	Years Since Injury	Injury Level
1	M	33	13	T4
2	F	26	9	T5/6
3	M	43	4	T8
4	F	54	25	L4
5	M	39	15	T5/6
6	M	34	1.5	L1
7	M	48	1	T4
8	F	63	24	T11/12
9	M	57	10	T10

6.2 Kinematic Data collection

Subjects were seated in their own wheelchairs which were positioned at a 135° angle from an adjustable tub bench as shown in Figure 25. The tub bench was adjusted to be level with the subject's wheelchair seat. Passive reflective markers were placed on the subject's C7 vertebrae, 3rd metacarpalphalangeal (3MP) joint, radial and ulnar styloid processes (RS and US respectively), and lateral epicondyle (LE) (see Figure 26). Markers were also placed on the subject's non-dominant hand and arm. Therefore all analyses

were limited to non-dominant arm. Subjects were then asked to transfer to the adjacent level tub bench, leading with their non-dominant hand, and subsequently back to their wheelchair. This was repeated three times. The coordinates of the hand position were recorded based on a global reference frame (shown in Figure 25) using a three-dimensional motion capture system (Qualisys MCU240, Qualisys Medical AB). Data were recorded at 120 Hz for 30 seconds.

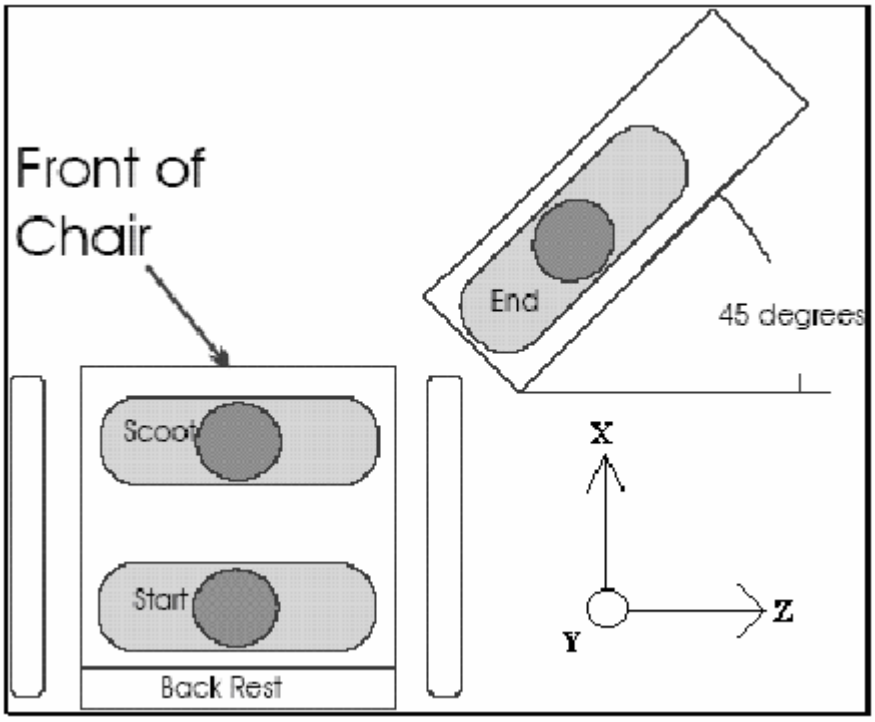

Figure 25 Illustration of experimental setup

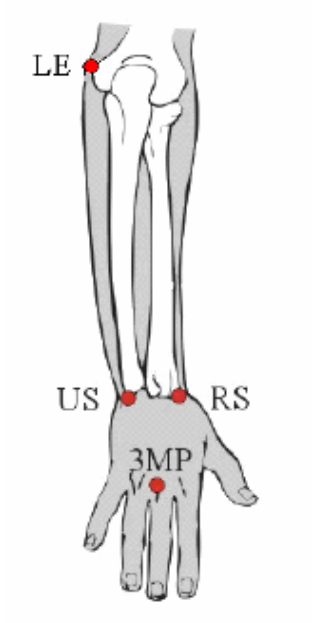

Lateral epicondyle (LE)
3rd metacarpal phalangeal (3MP)
Radial styloid (RS)
Ulnar styloid (US)

Figure 26. Anatomical points for kinematic marker placement on the hand, wrist, and arm.

6.3 Data Analysis

The motion data collected (see Section 6.2) were used to determine the peak joint forces and moments using dynamic force analysis, which is implemented using Matlab (see APPENDIX S). The dynamic force analysis explained in Section 6.3.1 was applied only during the transfer phase from the wheelchair to the tub bench and from the tub bench to the wheelchair. The method used in determining the transfer phase is explained in Section 6.3.2. The peak forces and moments at the joints during the transfer phase were then determined, which is discussed in 6.3.3.

6.3.1 Finding Joint Forces and Moments using Dynamic Force Analysis

The forces and moments at the wrist, elbow, and shoulder were determined using the concepts of dynamic analysis used in linkage mechanisms(30;31). Here hand, forearm, and upper arm are considered as three members of the linkage mechanism. Figure 27 shows the schematic diagram of the left arm with the salient marker points used in the model: thirdmp (t), wrist (w), elbow (e), and shoulder (s). Wrist, elbow, and shoulder joint centers were replaced with the radial styloid, olecranon, and acromion marker coordinates respectively.

The assumptions made during the dynamic force analysis are briefly described here. The body segments are considered as straight line rigid members (see Figure 27), i.e., the center of mass of the segments does not move relative to the joints. The joints can resist both forces and moments in 3D (i.e. ball-and-socket joint with friction). The joints centers were simplified by using the marker coordinates as stated in the above paragraph.

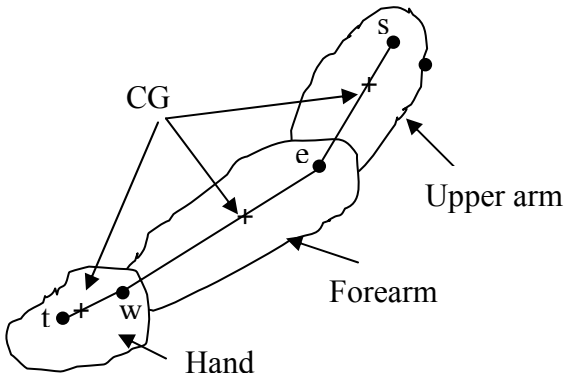

Figure 27 Schematic diagram of left arm with salient marker points

The mass of the body segments of the arm(i.e., upper arm, forearm, and hand) are calculated using anthropometric data (refer Table 3.1, page 56 of (32)). Let "M" be the total mass of the body. Then the mass of the body segments are given by Equation 1.

$$m_{ua} = M \cdot 0.028$$

$$m_{fa} = M \cdot 0.016 \qquad \text{Equation 1}$$

$$m_{ha} = M \cdot 0.006$$

m_{ua}, m_{fa}, and m_{ha} are the mass of the upper arm, forearm, and hand respectively.

The moment of inertia of the body segments is calculated by multiplying mass of the body segments by the square of the radius of gyration (refer Table 3.1, page 56 of (32)).

$$MOI_{ua} = m_{ua} \cdot 0.322^2$$

$$MOI_{fa} = m_{fa} \cdot 0.303^2 \qquad \text{Equation 2}$$

$$MOI_{ha} = m_{ha} \cdot 0.297^2$$

The linear velocity of the marker points are calculated using the finite difference method. In particular, backward difference is used, which is given in Equation 3.

$$v_{t\_i} = \frac{x_{t\_i} - x_{t\_i-1}}{\Delta t}$$

$$v_{w\_i} = \frac{x_{w\_i} - x_{w\_i-1}}{\Delta t}$$

$$v_{e\_i} = \frac{x_{e\_i} - x_{e\_i-1}}{\Delta t}$$

$$v_{s\_i} = \frac{x_{s\_i} - x_{s\_i-1}}{\Delta t}$$ Equation 3

Where Δt is time interval, 1/120 sec, between two consecutive position readings (represented by subscript 'i' and 'i-1') of the markers, *x* represents the position vector of the markers, and subscripts t, w, e, and s represents thirdmp, wrist, elbow, and shoulder (see Figure 27). Here for wrist is defined by position of radial styloid.

The linear acceleration at the marker points is calculated using central difference formula(33) and is given by Equation 4.

$$a_{t\_i} = \frac{x_{t\_i-1} - 2x_{t\_i} + x_{t\_i+1}}{\Delta t^2}$$

$$a_{w\_i} = \frac{x_{w\_i-1} - 2x_{w\_i} + x_{w\_i+1}}{\Delta t^2}$$

$$a_{e\_i} = \frac{x_{e\_i-1} - 2x_{e\_i} + x_{e\_i+1}}{\Delta t^2}$$

$$a_{s\_i} = \frac{x_{s\_i-1} - 2x_{s\_i} + x_{s\_i+1}}{\Delta t^2}$$ Equation 4

The angular velocity ω of body segment is determined using relative linear velocity and position between proximal and distal marker points as given in Equation 5.

$$v_{t\_w} = v_t - v_w$$

$$x_{t\_w} = x_t - x_w$$

$$\omega_{ha} = \frac{x_{t\_w} \times v_{t\_w}}{\left\| x_{t\_w} \right\|^2}$$

Equation 5

Similarly ω_{fa} and ω_{ua} are calculated as below.

$$\omega_{fa} = \frac{x_{w\_e} \times v_{w\_e}}{\left\| x_{w\_e} \right\|^2}$$

$$\omega_{ua} = \frac{x_{e\_s} \times v_{e\_s}}{\left\| x_{e\_s} \right\|^2}$$

The angular acceleration α of body segments is calculated using forward difference formula(33) as given in Equation 6.

$$\alpha_{ha\_i} = \frac{\omega_{ha\_i+1} - \omega_{ha\_i}}{\Delta t}$$

$$\alpha_{fa\_i} = \frac{\omega_{fa\_i+1} - \omega_{fa\_i}}{\Delta t}$$

$$\alpha_{ua\_i} = \frac{\omega_{ua\_i+1} - \omega_{ua\_i}}{\Delta t}$$

Equation 6

The inertia force assumed to act at the center of gravity of the body segment is calculated using Newton's second law (34) as given in Equation 7.

$$\overline{f}_{ha} = -\overline{a}_{ha} \cdot m_{ha}$$

$$\overline{f}_{fa} = -\overline{a}_{fa} \cdot m_{fa}$$

$$\overline{f}_{ua} = -\overline{a}_{ua} \cdot m_{ua}$$ Equation 7

where, $\overline{a}$ represents the acceleration about the center of gravity of the body segments. This is calculated using anthropometric data (refer Table 3.1, page 56 of (32)) as follows.

$$\overline{a}_{ha} = 0.494 \cdot a_w + 0.506 \cdot a_t$$

$$\overline{a}_{fa} = 0.570 \cdot a_e + 0.430 \cdot a_w$$

$$\overline{a}_{ua} = 0.564 \cdot a_s + 0.436 \cdot a_e$$

where, the constants represent the ratio of distance from center of mass to proximal/distal marker coordinate, to distance between the proximal and distal marker points (refer page 56 of (32)). Note that here position is twice differentiated to obtain the acceleration at the centroid.

The inertia moment is calculated similar to inertia force as given in Equation 8.

$$\overline{T}_{ha} = -\alpha_{ha} \times MOI_{ha}$$

$$\overline{T}_{fa} = -\alpha_{fa} \times MOI_{fa}$$

$$\overline{T}_{ua} = -\alpha_{ua} \times MOI_{ua}$$ Equation 8

Now the free body diagram of the hand, forearm and upper arm are analyzed to find the joint forces at the wrist, elbow, and shoulder.

6.3.1.1 Free body diagram of hand

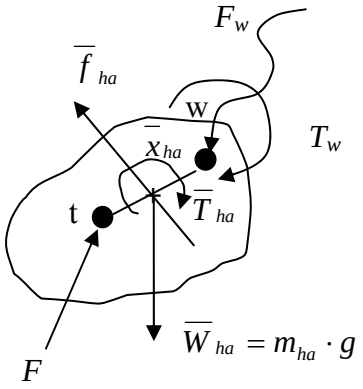

Figure 28 Free body diagram of Hand

The force at wrist Fw is calculated using the force equilibrium equation as given by Equations 9 and 10 (see Figure 28).

$$\sum_{i=1}^{N} F_i = 0$$ Equation 9

$$F_w = -(\overline{W}_{ha} + \overline{f}_{ha} + F)$$ Equation 10

In Equation 10 the formula is derived assuming single point load acting at the hand. The external force F acting on the hand was not measured but was estimated as 54.84% and 78.84% of body weight during wheelchair to tub bench (leading arm force) and tub bench to wheelchair (trailing arm force) transfer respectively. Here the external forces were assumed to be constant through out the entire transfer time. However, in practice external forces varies over time but external force was not directly measured. We chose to use the estimated maximum force in order to later identify the peak joint forces and moments during the transfers.

Applying moment equilibrium about the center of mass of the hand we can compute the moment at the wrist Tw as given by Equations 11 to 12.

$$\sum_{i=1}^{N} T_i = 0$$

Equation 11

$$T_w = -(\overline{T}_{ha} + ((x_w - \overline{x}_{ha}) \times F_w) + ((x_t - \overline{x}_{ha}) \times F))$$

Equation 12

6.3.1.2 Free body diagram of forearm

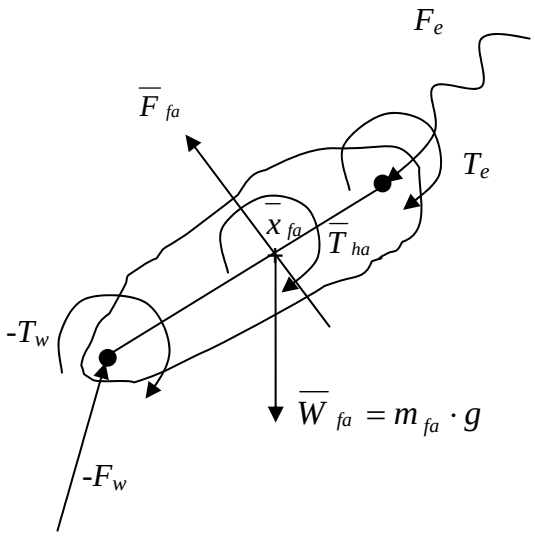

Figure 29 Free body diagram of Forearm

The force at the elbow Fe is calculated using the force equilibrium equation as given by Equations 13 and 14.

$$\sum_{i=1}^{N} F_i = 0 \quad \text{at forearm} \qquad \text{Equation 13}$$

$$F_e = -(\overline{W}_{fa} + \overline{f}_{fa} - F_w) \qquad \text{Equation 14}$$

Applying moment equilibrium about the center of mass of the forearm we can compute the moment at the elbow Te as given by Equations 15 and 16.

$$\sum_{i=1}^{N} T_i = 0 \qquad \text{Equation 15}$$

$$T_e = -(\overline{T_{fa}} - T_w + ((x_e - \overline{x_{fa}}) \times F_e) + ((x_w - \overline{x_{fa}}) \times -F_w)) \qquad \text{Equation 16}$$

6.3.1.3 Free body diagram of upper arm

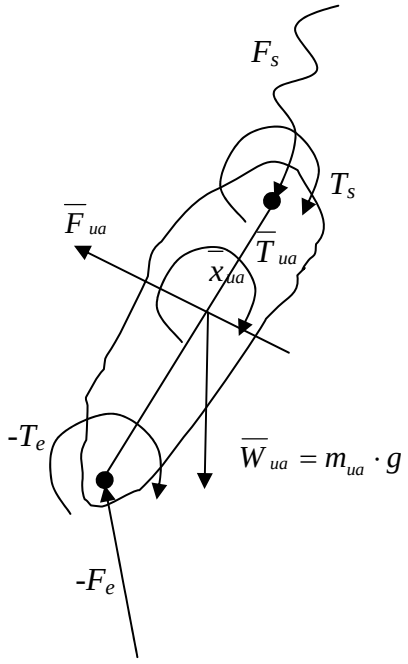

Figure 30 Free body diagram of Forearm

The force at the shoulder Fs is calculated using force equilibrium equation as given by Equations 17 and 18 (see Figure 30).

$$\sum_{i=1}^{N} F_i = 0 \quad \text{at upper arm} \qquad \text{Equation 17}$$

$$F_s = -(\overline{W}_{ua} + \overline{f}_{ua} - F_e) \qquad \text{Equation 18}$$

Applying moment equilibrium about center of mass of upper arm we can compute the moment at the shoulder Ts as given by Equations 19 and 20.

$$\sum_{i=1}^{N} T_i = 0$$

Equation 19

$$T_s = -(\overline{T_{ua}} - T_e + ((x_s - \overline{x_{ua}}) \times F_s) + ((x_e - \overline{x_{ua}}) \times -F_e))$$

Equation 20

6.3.2 Transfer Time

To determine the beginning and end of the transfer phase, the z-coordinate of the C7 vertebral marker was examined (20). This coordinate described the movement of the person in the horizontal direction when transferring from the wheelchair to the tub bench. Transfer-1, represents the subject transferring from the wheelchair to the tub bench (Figure 31). As force plate information was not available, it is defined by the initial change in trunk position to when the trunk position became stable. Transfer-2 represents the subject transferring from the tub bench back to the wheelchair. This is defined by the subsequent change in trunk position denoted by an increase in the curve to when the trunk reached its initial position. Figure 31 illustrates how the C7 marker was used to determine the duration of Transfer-1 and Transfer-2.

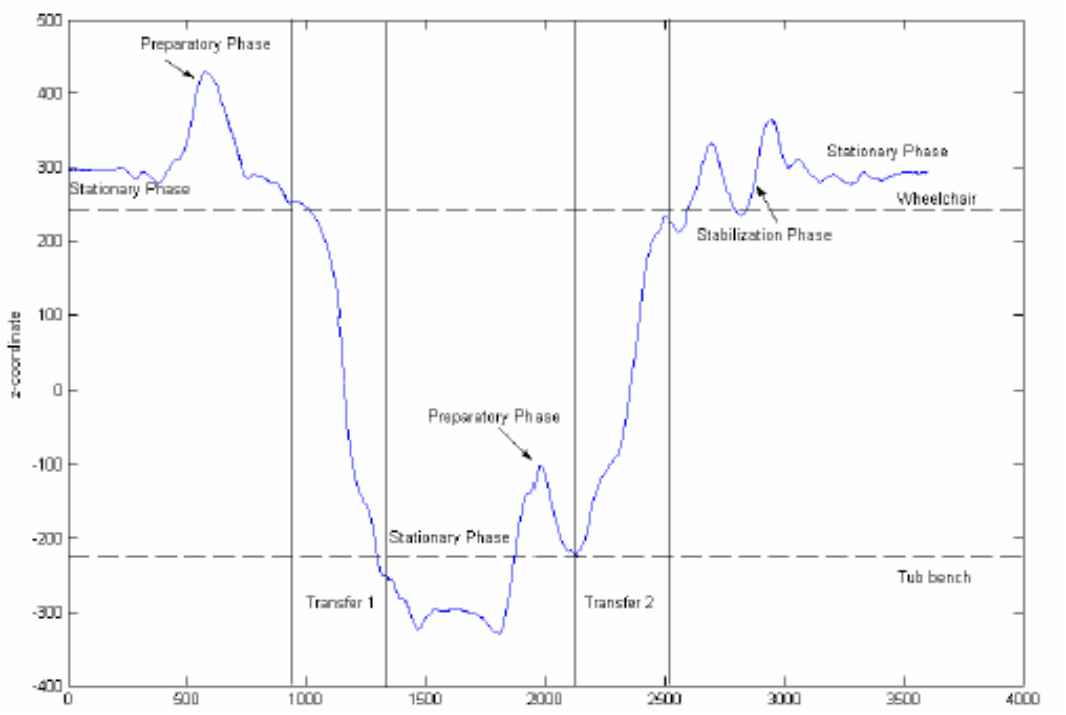

Figure 31 Z-coordinate position of the C7 vertebral marker and different transfer phases

6.3.3 Determining the Peak Forces and Moments at the Joints

The peak maximum forces and moments at the joints over the transfer from the wheelchair to the tub bench and from the tub bench to the wheelchair are given below.

$$\mathbf{V1_{max} = max \{||V_i|| \mid i = wt_1 \text{ to } wt_2\}}$$

Equation 21

Where, V1 represents any joint force or moment, and wt_1 and wt_2 represent the initial and final time during the transfer phase from the wheelchair to the tub bench.

$$V2_{max} = \max \{||V_i|| \mid i = tw_1 \text{ to } tw_2\}$$

Equation 22

Where, V2 represents any joint force or moment. tw_1 and tw_2 represent the initial and final time during the transfer phase from the tub bench to the wheelchair.

Peak forces and moments for wrist, elbow, and shoulder were calculated for transfer from wheelchair to tub bench and back. These data were determined for each of the three trials and averaged. These parameters were all computed using Matlab (Mathworks, Inc., Natwick, MA).

All trials of subject 2, 3, 4, and 5 were not used because of marker dropout during transfers.

6.3.4 Statistical Analysis

A paired t-test was performed to compare the joint forces for the leading arm (transfer to the tub bench) and trailing arm (transfer to the wheelchair). An 'α'of less than 0.050 was considered significantly different. Pearson Correlations were performed to see the correlation across the forces and moments with transfer time. A significance of p less than 0.05 was considered significantly correlated. All statistics were performed in the SPSS statistical package (SPSS, Inc., Chicago, Illinois)

7 RESULTS

Table 7 Peak resultant joint forces and moments during transfer from the wheelchair to the tub bench (leading arm)

Subject	Trial	RF wrist(N)	RM wrist(Nm)	RF elbow(N)	RM elbow(Nm)	RF Shoulder(N)	RM Shoulder(Nm)
1	1	350.84	57.86	357.08	76.02	405.14	112.07
	2	350.23	54.44	348.47	63.47	349.31	102.55
	3	349.23	52.15	400.14	64.27	508.23	141.73
	Mean	350.10	54.82	368.56	67.92	420.89	118.78
	SD	0.81	2.87	27.69	7.02	80.62	20.44
2	1	320.70	111.64	344.88	73.56	347.10	90.22
	2	320.09	83.66	354.39	80.81	436.52	103.30
	Mean	320.39	97.65	349.64	77.18	391.81	96.76
	SD	0.44	19.79	6.73	5.13	63.22	9.25
3	1	427.68	52.15	497.27	95.58	678.62	157.06
	2	415.24	30.95	423.76	99.88	474.40	120.33
	Mean	421.46	41.55	460.52	97.73	576.51	138.70
	SD	8.80	14.98	51.98	3.04	144.40	25.97
4	1	447.77	119.67	437.02	104.12	479.79	111.40
	2	432.98	142.87	439.46	90.19	513.08	130.84
	Mean	440.37	131.27	438.24	97.16	496.44	121.12
	SD	10.46	16.41	1.72	9.85	23.54	13.75
5	1	388.20	75.79	546.21	127.32	807.33	206.96
	2	415.67	174.12	500.60	76.10	558.44	143.48
	Mean	401.93	124.95	523.41	101.71	682.89	175.22
	SD	19.42	69.53	32.25	36.22	175.99	44.89
6	1	365.71	30.66	363.83	40.90	360.05	104.36
	2	393.93	229.64	533.93	76.47	504.61	140.97
	3	368.94	49.46	374.86	57.02	422.03	109.95
	Mean	376.19	103.25	424.21	58.13	428.90	118.43
	SD	15.45	109.86	95.18	17.81	72.52	19.72
7	1	492.81	109.56	531.35	67.44	535.05	163.80
	2	495.47	55.41	594.92	82.11	774.22	213.55
	3	478.04	95.16	509.89	76.19	526.22	159.20
	Mean	488.77	86.71	545.39	75.25	611.83	178.85
	SD	9.39	28.05	44.22	7.38	140.70	30.14
8	1	513.48	92.45	528.19	126.42	519.38	149.33
	2	504.08	74.08	523.05	86.74	514.85	154.89
	3	508.54	65.23	553.11	70.97	612.34	167.58
	Mean	508.70	77.25	534.78	94.71	548.86	157.27
	SD	4.70	13.88	16.08	28.57	55.03	9.35
9	1	442.53	59.48	475.98	113.04	560.22	179.43
	2	445.34	46.56	495.20	108.68	594.89	183.49
	3	438.46	34.21	521.08	115.47	667.80	191.95
	Mean	442.11	46.75	497.42	112.40	607.63	184.96
	SD	3.46	12.64	22.63	3.44	54.91	6.39

Table 8 Peak resultant joint forces and moments during transfer from the tub bench to the wheelchair. (trailing arm)

Subject	Trial	RF wrist(N)	RM wrist(Nm)	RF elbow(N)	RM elbow(Nm)	RF Shoulder(N)	RM Shoulder(Nm)
1	1	507.17	57.86	519.01	107.54	561.71	165.80
	2	505.82	57.73	540.75	161.48	601.71	231.24
	3	504.57	52.15	530.45	102.77	594.52	172.81
	Mean	505.85	55.92	530.07	123.93	585.98	189.95
	SD	1.30	3.26	10.87	32.61	21.33	35.93
2	1	453.01	342.49	535.29	305.11	537.99	333.45
	2	451.71	108.76	468.04	130.23	470.18	197.57
	Mean	452.36	225.63	501.67	217.67	504.09	265.51
	SD	0.92	165.27	47.56	123.65	47.95	96.08
3	1	623.25	362.62	922.78	274.54	915.26	217.08
	2	628.80	86.70	708.07	195.50	685.84	225.64
	Mean	626.02	224.66	815.43	235.02	800.55	221.36
	SD	3.93	195.10	151.82	55.89	162.22	6.05
4	1	594.62	151.10	713.51	216.75	903.24	292.64
	2	594.85	142.87	656.65	147.34	766.12	241.33
	Mean	594.73	146.99	685.08	182.05	834.68	266.98
	SD	0.16	5.82	40.20	49.08	96.96	36.28
5	1	571.54	97.58	864.88	180.64	1350.16	327.01
	2	577.60	174.12	640.76	239.45	776.53	286.69
	Mean	574.57	135.85	752.82	210.04	1063.35	306.85
	SD	4.28	54.12	158.48	41.59	405.62	28.51
6	1	527.97	36.78	535.82	111.76	652.57	151.63
	2	527.23	229.64	533.93	154.34	548.13	202.45
	3	544.48	125.52	585.21	163.34	674.03	243.64
	Mean	533.22	130.65	551.65	143.15	624.91	199.24
	SD	9.75	96.53	29.08	27.56	67.35	46.09
7	1	691.87	109.56	768.15	216.72	909.63	305.79
	2	698.78	108.57	719.82	238.71	774.22	302.31
	3	686.16	95.16	819.13	234.36	1033.24	327.10
	Mean	692.27	104.43	769.03	229.93	905.70	311.73
	SD	6.32	8.04	49.66	11.64	129.56	13.42
8	1	717.13	101.27	741.37	278.05	907.53	311.82
	2	733.38	125.23	783.17	289.02	819.64	297.87
	3	723.81	121.41	755.19	221.21	804.57	287.51
	Mean	724.78	115.97	759.91	262.76	843.91	299.06
	SD	8.17	12.88	21.29	36.40	55.60	12.20
9	1	641.78	69.57	655.68	198.13	713.88	215.56
	2	656.95	102.41	742.36	194.16	738.57	219.13
	3	635.76	74.77	662.09	233.50	735.99	271.57
	Mean	644.83	82.25	686.71	208.60	729.48	235.42
	SD	10.92	17.65	48.30	21.66	13.57	31.36

Table 9 Paired sample test results for mean peak net joint dynamic forces values comparing transfer from wheelchair to tub bench and tub bench to wheelchair. Group means and standard deviations are in parentheses.

Mean Peak RF	WC to TB(leading arm force in N)	TB to WC(Trailing arm force in N)	Significance (2-tailed)
Wrist	416.16(61.70)	594.29(88.22)	0.000
Elbow	460.24(71.23)	672.48(116.33)	0.000
Shoulder	529.52(100.6)	765.85(173.9)	0.000

Table 10 Paired sample test results for mean peak net joint dynamic moment values comparing transfer from wheelchair to tub bench and tub bench to wheelchair. Group means and standard deviations are in parentheses.

Mean Peak Moment	WC to TB(leading arm moment in Nm)	TB to WC(Trailing arm moment in Nm)	Significance (2-tailed)
Wrist	84.91(32.70)	135.81(57.81)	0.039
Elbow	86.97(17.88)	201.46(44.53)	0.000
Shoulder	143.34(31.84)	255.12(46.04)	0.000

Table 9 shows the results of the t-test analysis. All mean peak net joints forces were significantly larger in trailing arm than the leading arm. Table 10 shows all mean peak net joints moments were significantly larger in trailing arm than the leading arm However, here we were comparing two different transfers (i.e wheelchair to tub bench transfer and tub bench to wheelchair transfers)

Table 11 Pearson Correlation for peak joint forces with transfer time

Peak joint force with time to transfer	r value	Sig. (2-tailed)
Wrist and time WC to TB	-0.69	0.042
Wrist and time TB to WC	-0.28	0.468
Elbow and time WC to TB	-0.40	0.292
Elbow and time TB to WC	0.18	0.650
Shoulder and time WC to TB	-0.19	0.628
Shoulder and time TB to WC	0.37	0.330

In wheelchair to tub bench transfer, there was a inverse relationship between wrist forces and transfer times (r = - 0.69, p = 0.042)(Table 11). Wrist forces with transfer times were not correlated during tub bench to wheelchair transfer. Elbow and shoulder forces with transfer times were not correlated during transfers.

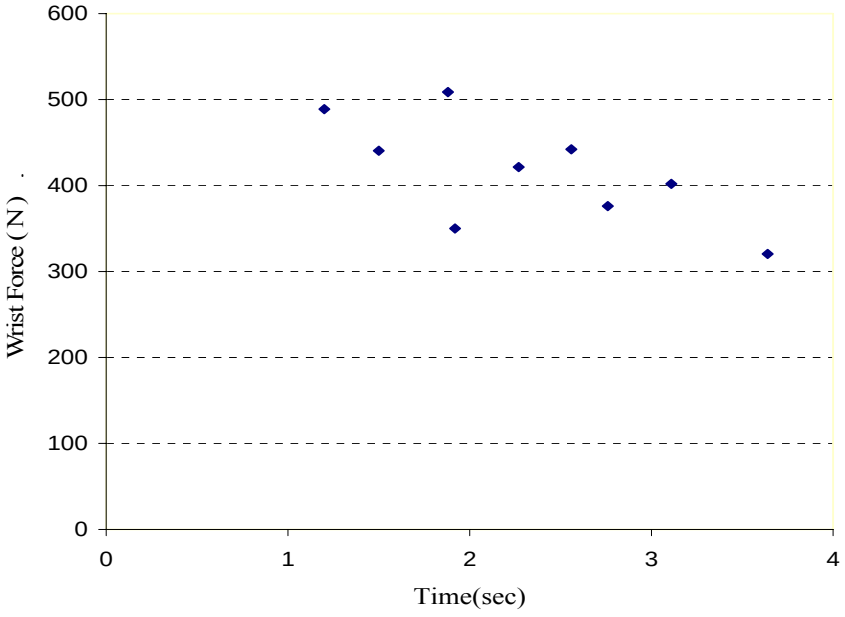

Figure 32 Peak wrist forces with transfer time during the wheelchair to the tub bench transfer (r = -0.69, p = 0.042).

Table 12 Pearson Correlation for peak joint moments with transfer time

Peak joint moment with time to transfer	r value	Sig. (2-tailed)
Wrist and time WC to TB	0.12	0.755
Wrist and time TB to WC	0.58	0.099
Elbow and time WC to TB	0.01	0.974
Elbow and time TB to WC	0.24	0.542
Shoulder and time WC to TB	-0.28	0.473
Shoulder and time TB to WC	0.30	0.433

Moments with transfer times were not correlated during wheelchair to tub bench and tub bench to wheelchair transfers (Table 12).

Table 13. Time for Transfers to and from Tub Bench. Standard deviations are in parentheses.

Subjects	Time to transfer fromWC to TB	Time to transfer from TB to WC
1	1.92 (-0.2)	2.33 (-0.75)
2	3.64 (-0.54)	3.94 (-0.44)
3	2.27 (-0.05)	3.88 (-0.6)
4	1.5 (-0.49)	2.84 (-0.11)
5	3.11 (-0.27)	5.11 (-2.01)
6	2.76 (-0.5)	3.43 (-0.79)
7	1.2 (-0.23)	2.92 (-0.2)
8	1.88 (-0.27)	2.73 (-0.05)
9	2.56 (-0.54)	2.76 (-0.76)
Total	2.32 (-0.78)	3.33 (-0.86)

8 DISCUSSION

The primary purpose of this study was to analyze the joint forces and moments during level tub bench transfers in persons with paraplegia. The mean peak net shoulder forces and moments were significantly greater in the trailing arm than that of the leading arm (see Table 7 and Table 8). The external force acted on the hand as the subjects pressed against the wheelchair or tub bench surfaces during both transfers. The peak forces were experienced when the subject was in between the wheelchair and the tub bench as shown graphically (Section 3.6.4); and hence the forces at the shoulder reached maximum value. In this transfer phase, subject shifted the body weight between the supporting extremities. Bayley et. al have reported that peak subacromial pressures were 2.5 times the arterial pressure during this phase of transfer in subjects with paraplegia(17)

Two related studies looked at muscle activity of the shoulder during wheelchair transfers (16;35). Although, methodologies were different, they reported greater peak EMG amplitude in the anterior deltoid and the serratus anterior muscle in the trailing arm than the leading arm during transfers (see table 1 and 2). The loaded extremity and needed stabilization placed a greater demand on the scapulothoracic muscles, as indicated by the increased activity of the lower trapezius and serratus anterior while the scapula was internally and downwardly rotated in the trail arm transfer.

Table 14 Comparison of the peak values during the loaded phase

of trailing arm, leading arm EMG amplitudes(%MVC)

	Trail arm	Lead arm
Biceps	24	22
Anterior deltoid	40	24
Serratus anterior	52	35

(Finely et al., 2005) n=23 males

Table 15 Comparison of the median values during lift phase

trailing arm, leading arm EMG amplitudes (%MVC)

	Trail arm	Lead arm
Biceps	23	28
Anterior deltoid	44	20
Serratus anterior	54	47

(Perry et al., 1996), n=12 males with SCI

Even though we cannot compare the EMG findings with forces calculated from inverse dynamics directly, an increase in muscle activities shows that muscles were working harder to stabilize the shoulder forces. Finely et al., found significant reduction in scapular upward rotation and posterior tip in trailing arm than the leading arm(35). Researchers(19;20) have found that reduction in scapular upward rotation and posterior tip reduces subacrominial space which leads to shoulder impingement and possibly increasing the potential for pathology . Note that in our study, increased shoulder joint forces were observed in trailing arm than in leading arm. The current study did not look

at the position of the arms. Position of the arms along with the joint forces may give a clearer idea of the mechanisms leading to shoulder impingement.

Similar to the observations made in shoulder forces and moments, peak net forces and moments at the elbow and wrist were significantly higher in trailing arm than leading arm (see Table 9 and Table 10). As per author's knowledge, no prior effort has been made to investigate elbow and wrist forces and moments during transfers.

Knowing the differences in leading and trailing arm forces with transfer time may assist in modifying transfer style in individuals with weakness, strength imbalance and shoulder pathologies. From a clinical perspective, even minor alterations in forces at the shoulder may be important for people with shoulder pathology. In wheelchair to tub bench transfer, inverse relationship between wrist forces and transfer times ($r = -0.69$, $p = 0.042$) was observed (i.e, less force was experienced while transferring slowly). A previous study by Butler et. al. using video images and 3-axis accelerometric data in car seat to wheelchair transfer, shows that transferring the body in multiple stages is safer than transferring in one movement (23). Therefore, it may be advisable to ask people to transfer slowly in multiple stages to minimize the shoulder forces.

For the wheelchair users with spinal cord injury (SCI), there was greater difference in time going one direction verses the other direction compared to the initial testing with design engineer. The time to transfer from the tub bench to the wheelchair was significantly greater than the time to transfer from the wheelchair to the tub bench(i.e,

the mean transfer time from wheelchair to tub bench for nine subjects with SCI was 2320ms(780 SD) and mean time to transfer from tub bench to wheelchair was 3330ms(860 SD)) (36). This could be due to level of experience, level of injury, use of non-dominant limb, and the added challenge of maneuvering back into the wheelchair.

During tub bench to wheelchair transfer, the mean peak net joint forces were not significantly correlated with transfer time during tub bench to wheelchair transfer. This could be because the subjects performed transfers using their own strategies in their wheelchairs and this may have introduced a lot of variability in the data. Although the instructions to subjects were standardized, the variation in wheelchairs and experience in transfers may also have contributed to the lack of correlation between force and transfer time.

The inverse dynamic analysis using serial linkage mechanism provides insight on ways to reduce the joint moments during transfer. When the person moves by having lower and upper arms close to horizontal direction, large moments may be experienced at proximal ends of the upper and lower arms due to increased moment arm. Similarly, when the lower and upper arms are close to vertical direction, less moment may be experienced at the proximal end of the upper and lower arms due to decreased moment arm. Anthropometry of the subjects may also influence joint forces and moments.

In the future, the method of inverse dynamic analysis used in this study can be used to simulate transfers in various arm positions to determine the best arm positions for

transfers that minimize the forces and moments at joints. Note that, unlike previous work (37), the current method considers the body weight, inertia forces, and moments. The best configuration can then be verified with subjects using the experimental setup developed.

A limitation of our study is that the forces exerted at the hand were not measured. The external force at the hand has been approximated as a constant 54.83% of the body weight during transfer from the wheelchair to the tub bench and a constant 78.84% of the body weight during tub bench to wheelchair transfer. This force was also based on Fz only not the individual force components. In the future, the actual external time varying force exerted at the hand needs to be measured. Currently, the body segments are assumed as rigid and the detailed muscle forces are not analyzed at the joints. In the future, a more advanced model needs to be developed to analyze the forces in different muscles at the joints.

Additionally, markers were placed on the subject's non-dominant arm. Subjects transferred to the tub bench leading with their non-dominant hand and subsequently back to their wheelchair. However, due to varied environments and obstacles, wheelchair users perform transfers daily, leading with either their dominant or non-dominant limb as needed.

9 SUMMARY

In this thesis, (1) a transfer measurement system was developed and evaluated for recording biomechanics of the upper limbs during four wheelchair transfers, (2) a new approach that objectively identifies the various phases of a wheelchair to tub bench transfer and back was determined (3) a method was developed for an inverse dynamic analysis of the upper limbs during a tub bench transfer. The details are briefly summarized in the following paragraphs.

A transfer system was developed for measuring kinematic and kinetic parameters of four wheelchair transfers, and it was tested by collecting data of a design engineer in the project. The four transfers included to-and-fro transfers between wheelchair and tub bench, wheelchair and tub bench using trapeze, wheelchair and toilet seat using grab bar, and wheelchair and car seat using overhead grab bar.

The evaluation process consisted of examining loadcell data, kinematic and force plate data. The phases of transfer were identified using both left and right force plate data and position and velocity of the marker C7. In the tub bench transfer, observations made by analyzing the sample collected data were: (1) forces in the trailing arm were more than leading arm, (2) the force coming on the leading and trailing arm as a percentage of body weight could be approximated. The observations were consistent with results published by other researchers, thus implying that the measurement system is likely effective.

This thesis identifies the weaknesses of the current measurement system and proposes changes in the design to improve the performance of measurement system. The weaknesses identified include, (1) in toilet seat transfer, fastener to hold side grab is functionally not very effective, (2) in car seat transfer; deflection of the overhead grab bar (which acts like cantilever beam) was seen. Some of the design changes include, (1) in toilet seat transfer, mounting side grab bar on the vertical wall using two load cells, (2) in car seat transfer, stabilizing the overhead grab bar by adding a truss member to reduce deflection.

In part II of the thesis, the peak joint forces and moments at wrist, elbow, and shoulder were determined by inverse dynamics in a level tub bench transfer of nine individuals with paraplegia. The proposed approach for inverse dynamics models the upper limbs as serial linkage mechanism. Unlike previous approaches, here body weight, inertia forces, and inertia moments of the body segments were considered into account. It was found that peak net joint forces were greater in the trailing arm than in the leading arm. There was an inverse relationship between wrist force and transfer time during wheelchair to tub bench transfer. Knowing the differences in leading and trailing arm forces with transfer time will assist in modifying transfer style in individuals with weakness, strength imbalance, and shoulder pathologies.

In the future, inverse dynamics can be used to identify the best way of transfer for clinical purpose. The best way of transfer can be determined using inverse dynamics by simulating the forces and moments at the joints during various arm positions. The best

way of transfer can then be verified using the transfer measurement system developed in this thesis.

APPENDIX A

Aluminium Mounting Plate

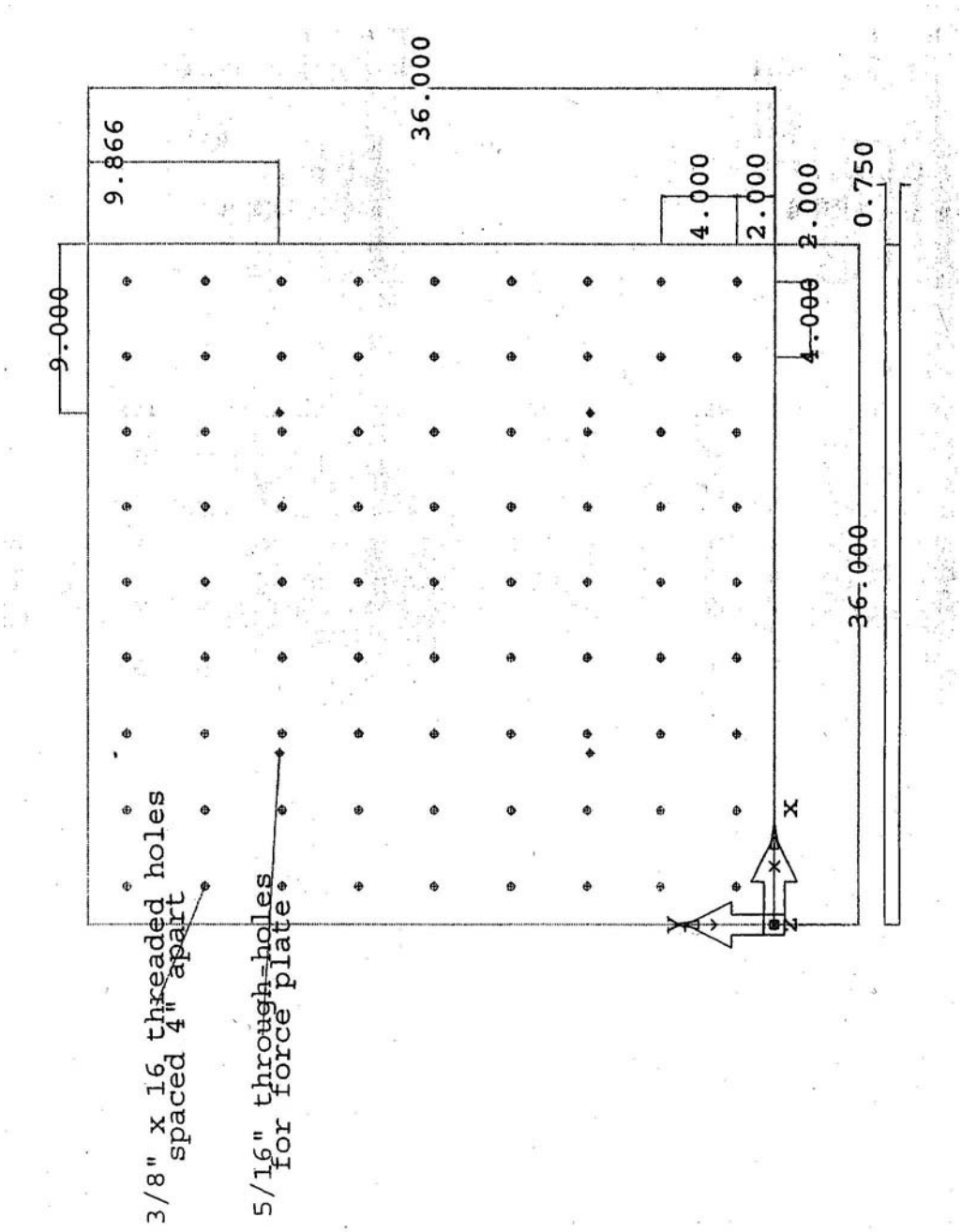

Handrail Housing

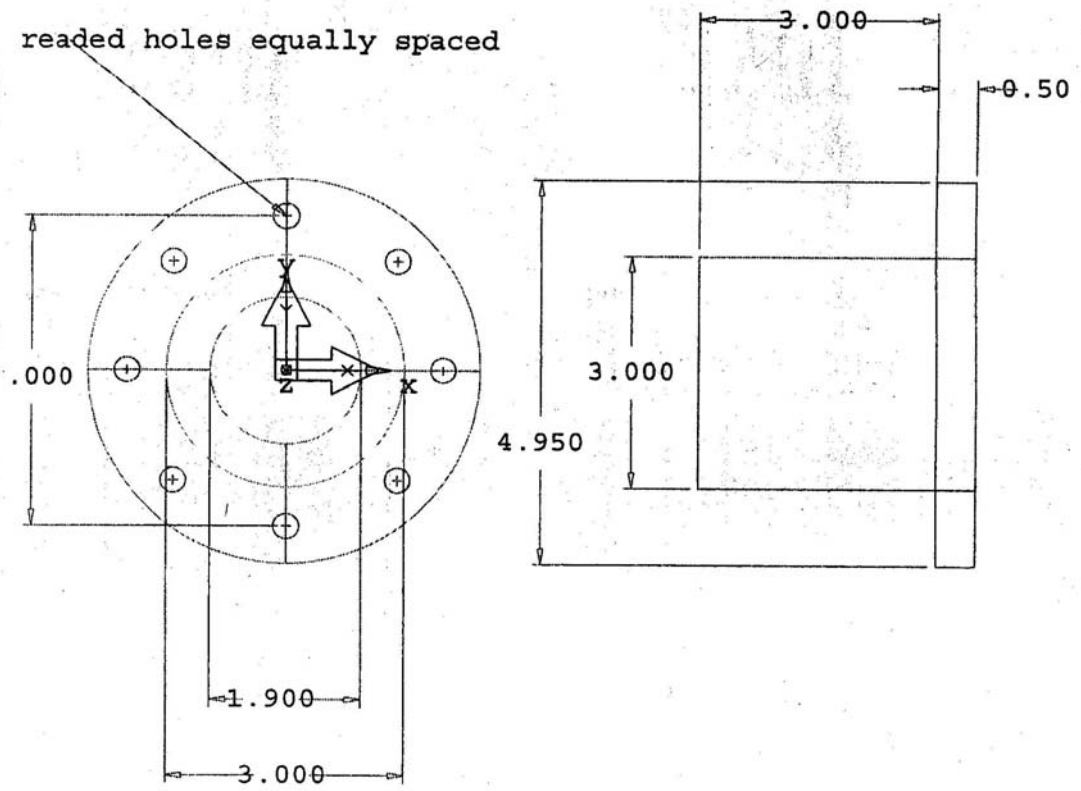

Steel Frame-Force plate apparatus

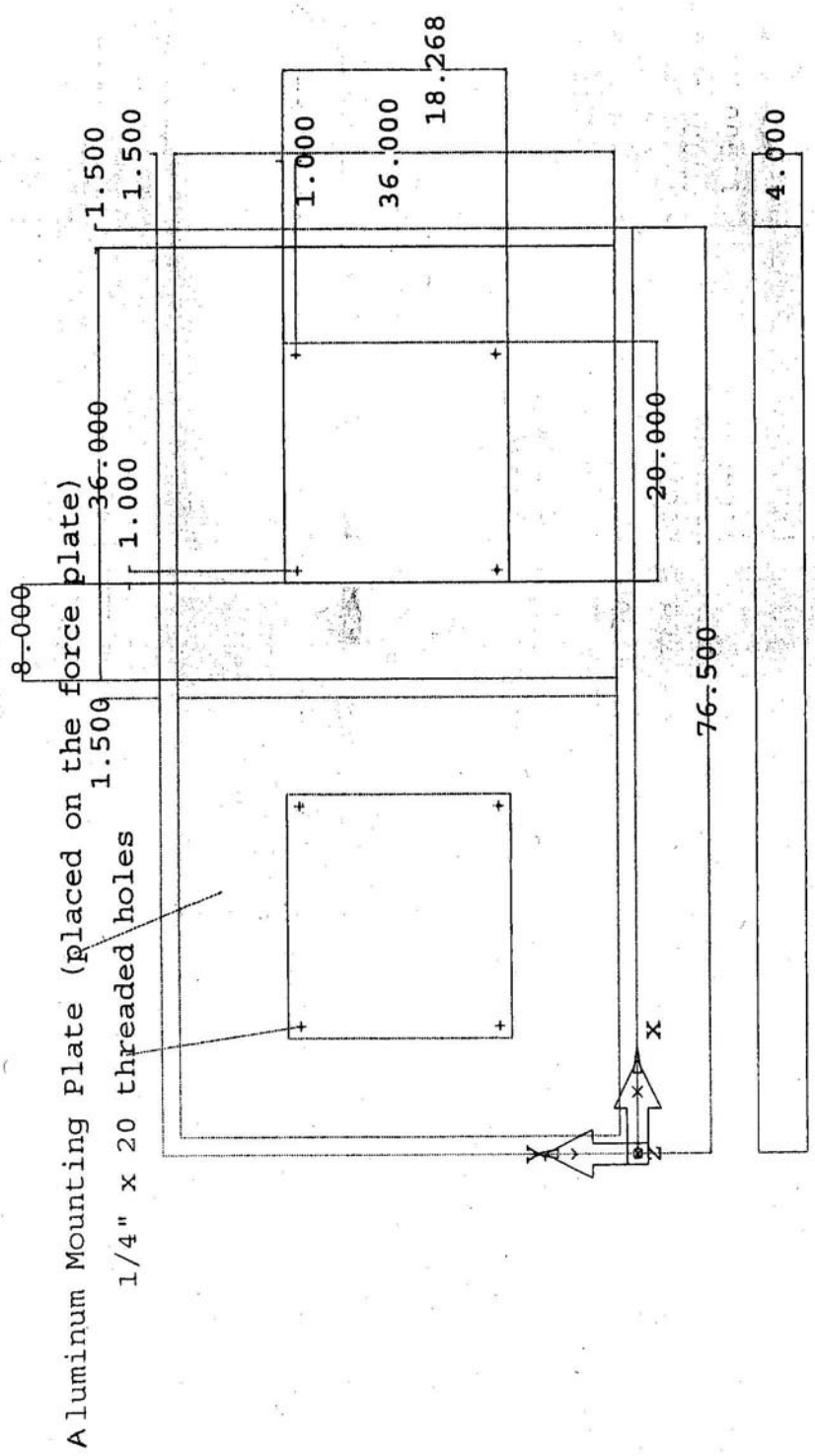

Load cell Grip

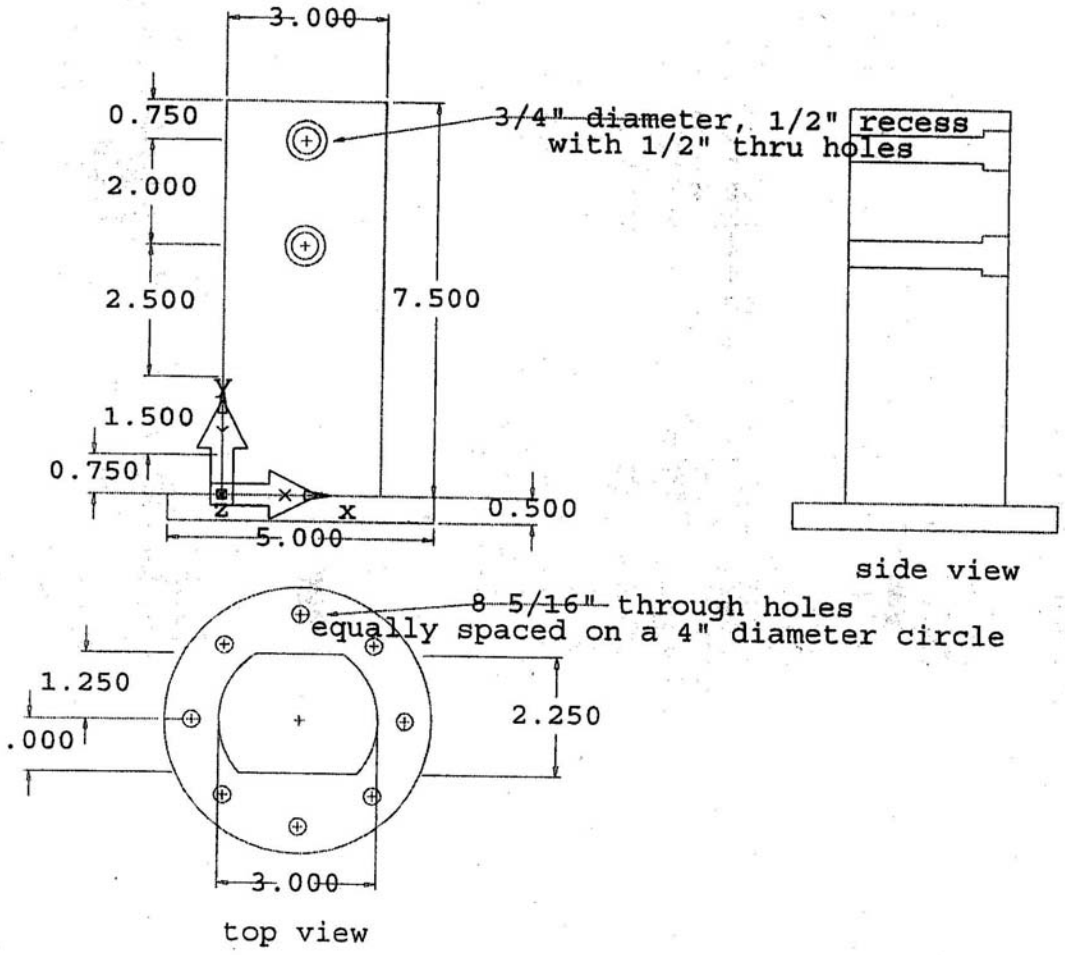
3.000
0.750
3/4" diameter, 1/2" recess
with 1/2" thru holes
2.000
2.500
7.500
1.500
0.750
Y
Z
X
0.500
5.000
side view
8 5/16" through holes
equally spaced on a 4" diameter circle
1.250
.000
2.250
3.000
top view

APPENDIX B

ADA side transfer Toilet setup

ADAAG FIGURE
TOILET STALLS
STANDARD STALL

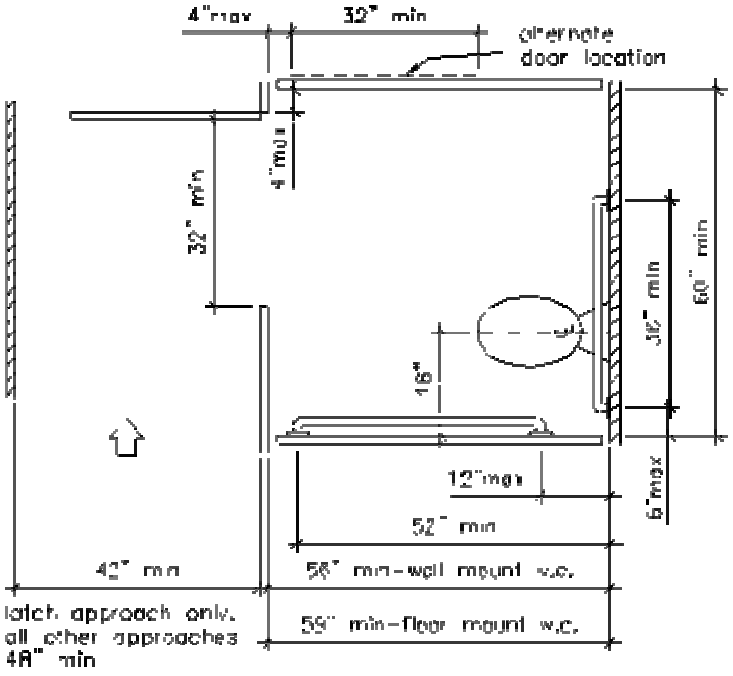

APPENDIX C

Car seat Securement

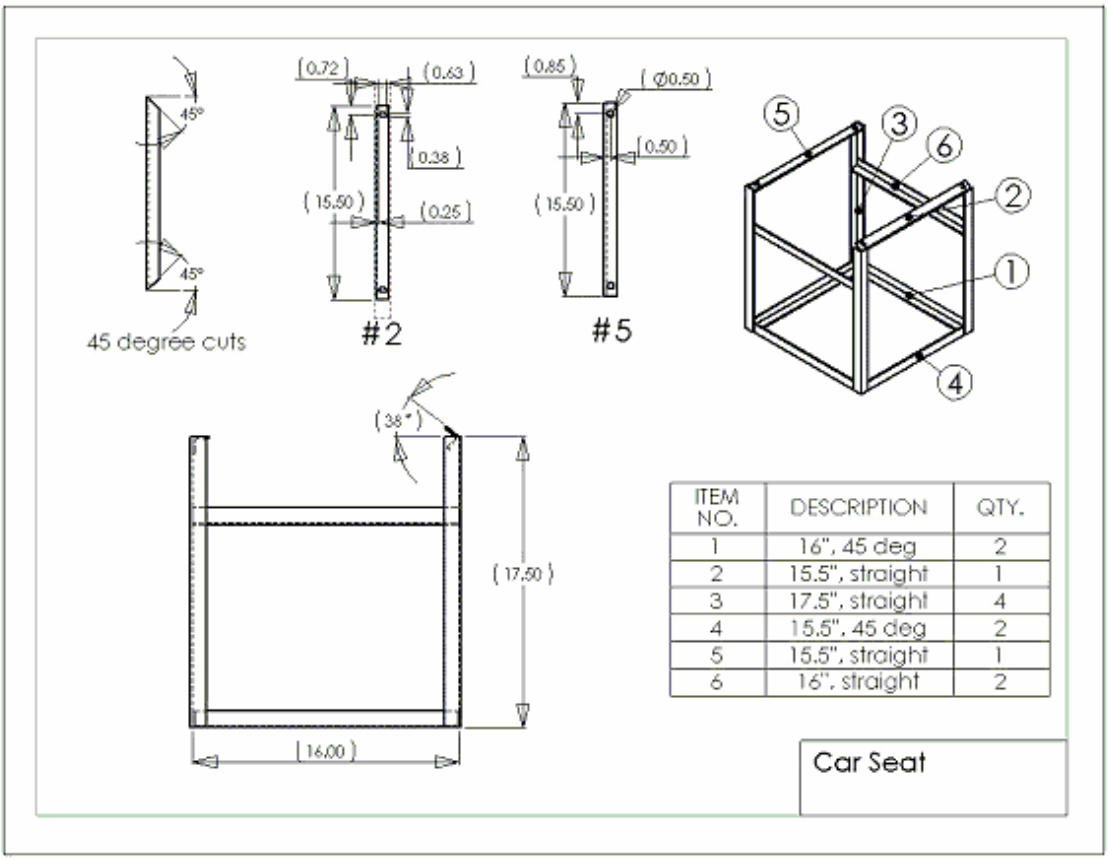

APPENDIX D

Loadcell.m

```
%this program loads in the load cell raw data files and converts the data
%to meaningful forces and moments based on the manufacturer provided calibration
matrix.
[file,file_path]=uigetfile('*.*', 'select a loadcell baseline file');
file_string=[file_path, file];
baseline= load(file_string);
[file,file_path]=uigetfile('*.*', 'select a loadcell data file');
file_string=[file_path, file];
loadcell= load(file_string);

Slc=[0.002020731985 0.0020175366068 0.0005446233169 0.031186239 0.030998617
0.030979161];
%sensitivity of the load cell

for i=1:6
for j=1:length(loadcell)
lc(j,i)=(loadcell(j,i)-baseline(j,i));% Making the data starts from zero
end;
end;

lc_n=lc(:,1:6);

for i=1:6
lc_n(:,i)=lc_n(:,i)/Slc(i);
end


[b,a]=butter(4,20/200);     %a 4th order butterworth digital filter is used to sample the
signal
                            %with a cutoff frequency of 20/200 Hz, where 200=half of
                            loadcell     % sampling rate
for i=1:6;
lc_n_filtered(:,i)=filtfilt(b,a,lc_n(:,i));
end;

Fxf=(lc_n_filtered(:,1));
Fyf=(lc_n_filtered(:,2));
Fzf=(lc_n_filtered(:,3));
Mxf=(lc_n_filtered(:,4));
Myf=(lc_n_filtered(:,5));
Mzf=(lc_n_filtered(:,6));

save lc_n_filtered lc_n_filtered  -ascii -tabs
```

APPENDIX E

OPTOTRAK Cameras Calibration Protocol

- Only to be re-calibrated if the cameras or dyno has been moved.
- Use one camera only when making a rigid body
- Use two cameras when registering cameras only

Calibration of Two Camera System

1. Connect the second camera, "slave."

2. In MS-DOS mode run "optsetup" from the C:*ndigital* prompt directory, which will create a new STANDARD.CAM in the REALTIME folder found under the *ndigital* folder.

3. Copy the STANDARD.CAM file from the C:\ REALTIME> directory to C:*ndigital* directory or folder.

4. Delete any of the existing *.CAM files in the *ndigital* folder.

5. Start the "Collect" program in windows.

6. Under "System" window, select "System Configuration."

7. Use the present rigid body on dyno for two-camera calibration.

8. Click on the windows icon and select "optotrak."

9. Select "Collection Parameters" in the "edit" menu and change the number of markers to 16 total.

10. Select "File Collection Parameters" in the "edit" menu and change trial to 1 and also specify a new file extension.

11. Change the length of collection to 60 seconds.

12. Go to "View" menu, choose "Alternative Display Options" and select 3D data.

13. Activate the markers by pressing F3 and select "View" under "Realtime Display."

14. Set up the 3D box where all of the markers can be seen by both cameras at the same time. Verify each marker position corresponds with the viewer .

15. When ready activate data collection by pressing "F4." Wave the 3D box in the capture volume in which you will be testing.

16. Create a new folder (ex. Koontz4) and copy: STANDARD.CAM, and R#001.XXX motion file for waving box, and the *3D box.rig* file.

17. Open MS-DOS prompt and type cd C:*ndigital*\folder name (koontz4)

18. Once in the directory type the following:
Register r#001.xxx box3d -istandard –ofilename (ex john2)

19. Copy new *.CAM file into the *ndigital* directory and delete STANDARD.CAM.

20. To create a Lab Coordinate System place three markers on the dyno:

For the Pink dyno:

a. Place #1 midway on the second drum along the axis of rotation.
b. Place #2 at the end of the roller out onto the carpet, along the axis of rotation. NOTE: markers #1 and #2 define the negative z-axis.
c. Place #3 along the vertical axis in the xz-plane. Note: this defines the direction of the x-axis.

For the Rear dyno:

a. Place #1 midway between the two rollers along the axis of rotation.
b. Place #2 at the end of the left roller along the axis of rotation. NOTE: markers #1 and #2 define the negative z-axis.
c. Place #3 somewhere on the dyno in the xz – plane. Note: this defines the direction of the x-axis.

21. Change the number of markers to three.

22. Collect 5-second data file of markers.

23. Convert to a C# file(Windows-optotrack-file-convertfile-r#*.*file that collected for5-second)

24. Run “Rigmaker” from the MS-DOS prompt command line.

25. Select “Build,” and use the “Static View Option.”
Load the 3D file just converted
Enter how many markers
Enter which marker to start at (most likely #1)
Change floating-point file to C#001XXX

26. Select TRANSFORM using ALIGNMENT PARAMETERS.
    Align the rigid body orientation you want
    Ie. Origin at marker #1, z-axis between #1 and #2, and marker #3 defining the xz-plane.

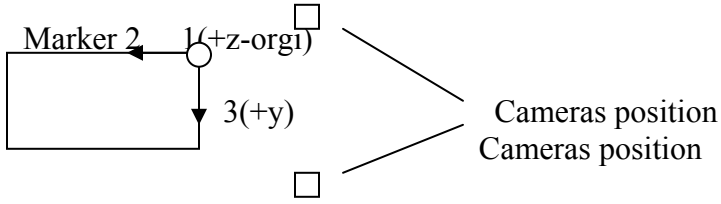

Alignment Parameters
Origin 1

Axis Marker	Coordinal plane markers
x-axis 2	XY plane 3
y-axis	XZ plane
z-axis	YZ plane

Alignment Parameters

27. A new Rigid File is created. Save and exit the program.

28. In windows explorer, copy the Rigid Body File over from *ndigital* / RIGID folder to the new folder (ex. Koontz4)

29. Go back to MS-DOS C:*ndigital*\file name (ex. koontz4)

30. Type the following:

    Align c#001.XXX XXX.rig -icam -odyno.
    C#001.XXX: 5 seconds of dyno marker data
    XXX.rig: rigid body file made on three markers
    -i.cam: camera calibration file *.cam used to collect the Rigid Body File.
    (ex: itemp)
    -odyno : new file name for dyno Lab coordinate system.

30. Copy new *.CAM file into *ndigital* and Delete the old*.cam file.

APPENDIX F

Kinematic Marker Placement

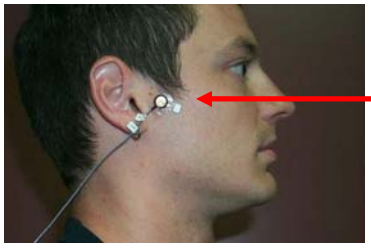

Tempero-mandibular joint

Lateral-superior border of the acromion

Lateral epicondyle

Tip of olecranon

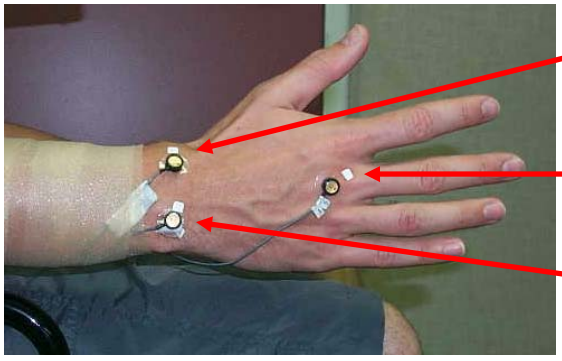

Radial styloid

Head of the 3rd metacarpal

Prominent tuberosity of the ulna

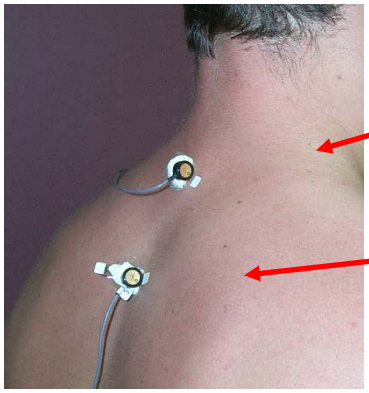

C7 spinous process

T3 spinous process

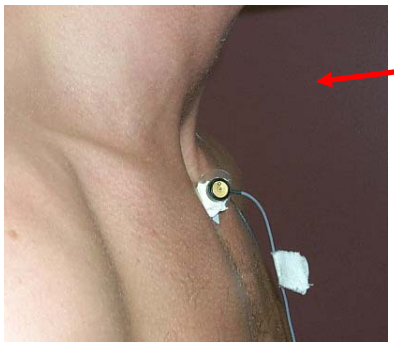

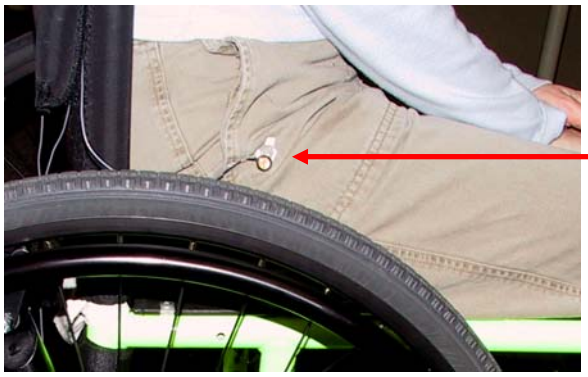

Marker Placement Protocol

1. Bilateral tempero-mandibular joints

Lateral-superior border of the acromion: Palpate the edge of the acromion and place a marker at the most lateral and superior portion of the edge of the acriomion

Lateral epicondyle: Palpate the lateral epicondyle with the subject in anatomical position, with arms fully extended. Place a finger on the lateral epicondyle and flex the elbow to 90°. Place a marker where your finger is.

Olecranon: Palpate the tip of the olecranon with the subject in anatomical position. Place a finger on the tip of the olecranon and flex the elbow to 90°. Place a marker where your finger is.

Radial styloid: Palpate the radial styloid with the subject in anatomical position

Prominent tuberosity of the ulna: Palpate the most prominent tuberosity of the ulna with the subject in anatomical position

3rd Metacarpal: Palpate the head of the 3rd Metacarpal with the subject's fingers and wrist fully extended

C7 Spinous process: Palpate C7 and place a marker facing LEFT camera

T3 Spinous process: Palpate T3 and place a marker facing LEFT camera

Sternum: Palpate the most superior portion of the sternum and place marker at the sternal notch facing LEFT camera

Hub: Place marker on the rotating pendulum attached to the SMART^{Wheel} Hub

Greater Trochanter: Palpate the greater trochanter and place marker in view of camera. If the hip marker is blocked, place the marker on wheelchair side guards or in a visible location, but record position relative to greater trochanter. Remove the marker after collecting the SETPO trial if it is occluded during propulsion or it inhibits propulsion.

APPENDIX G

OPTOTRAK Marker Placement for Car seat

Marker Number	Anatomical Landmark	Column # X	Column # Y	Columan # Z
1	Sternal Notch	2	3	4
2	C7	5	6	7
3	T3	8	9	10
4	Left TMJ	11	12	13
5	Left Acr	14	15	16
6	Left Lat. Ep.	17	18	19
7	Left Olecronon	20	21	22
8	Left Ulnar tub.	23	24	25
9	Rad. Sty.	26	27	28
10	3rd MP	29	30	31
11	Left Knee	32	33	34
12	Left hub	35	36	37
13	Left top of seat	38	39	40
14	Left side of Wheelchair	41	42	43
15	Left bottom of seat	44	45	46
16	Left caster	47	48	49
17	Grab bar base	50	51	52
18	Right top back of car seat	53	54	55
19	Right top front of car seat	56	57	58
20	Right bottom front of car seat	59	60	61
21	Left top front of car seat	62	63	64
22	Left middle of car seat back	65	66	67
23	Left top of car seat back	68	69	70
24	Grab bar free end	71	72	73
25	Grab bar at bend	74	75	76

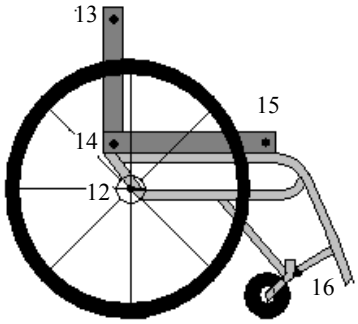

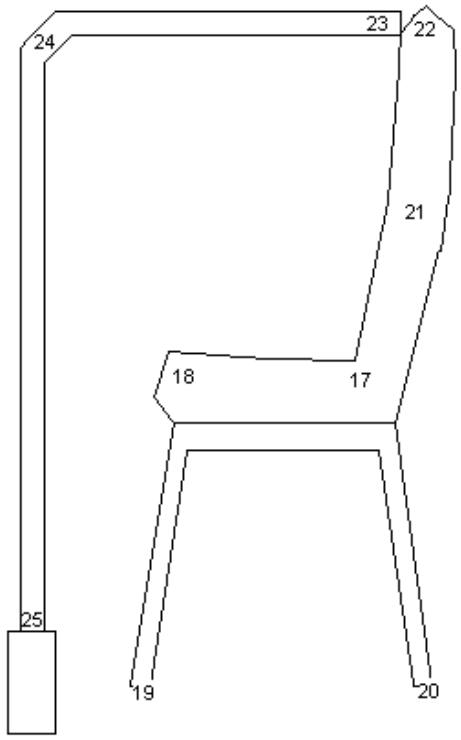

Diagram 1: Wheelchair **Diagram 2 : Car seat**

APPENDIX H

OPTOTRAK Marker Placement for Tub bench and Trapeze set up

Marker Number	Anatomical LandMarker	Column # X	Column # Y	Column # Z
1	Sternal Notch	2	3	4
2	C7	5	6	7
3	T3	8	9	10
4	Left TMJ	11	12	13
5	Left Acr	14	15	16
6	Left Lat. Ep.	17	18	19
7	Left Olecronon	20	21	22
8	Left Ulnar tub.	23	24	25
9	Rad. Sty.	26	27	28
10	3rd MP	29	30	31
11	Left Hub	32	33	34
12	Left Knee	35	36	37
13	Left top of seat	38	39	40
14	Left side of Wheelchair	41	42	43
15	Left bottom of seat	44	45	46
16	Left Caster	47	48	49
17	Top back corner of T.B.	50	51	52
18	Top front corner of T.B.	53	54	55
19	Bottom front right corner of TB	56	57	58
20	Top front left corner of TB	59	60	61

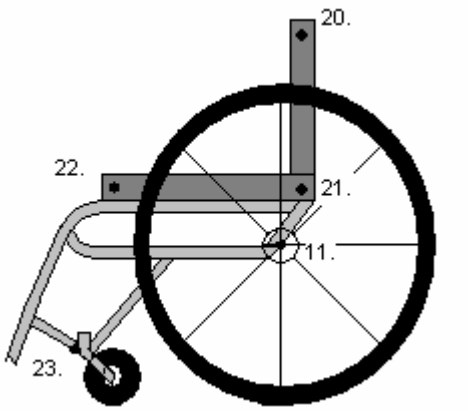

20. = 13, 21. = 14, 22. = 15, 23. = 16

Diagram 1: Wheelchair

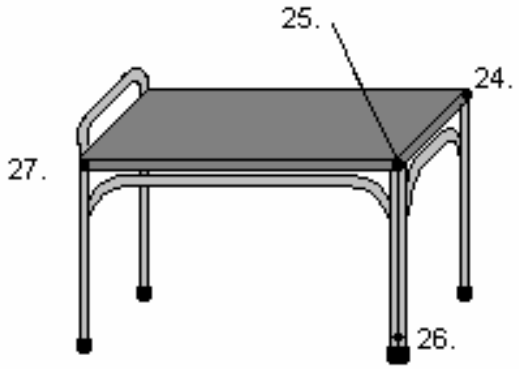

24 = 17, 25 = 18, 26 = 19, 27 = 20

Diagram 2: Tub bench

APPENDIX I

OPTOTRAK Marker Placement for Toilet seat

Marker Number	Anatomical Landmark	Column# in X	Column # in Y	Column # in Z
1	Sternal Notch	2	3	4
2	C7	5	6	7
3	T3	8	9	10
4	Left TMJ	11	12	13
5	Left Acr	14	15	16
6	Left Lat. Ep.	17	18	19
7	Left Olecronon	20	21	22
8	Left Ulnar tub.	23	24	25
9	Rad. Sty.	26	27	28
10	3rd MP	29	30	31
11	Left Hub	32	33	34
12	Left Knee	35	36	37
13	Left top of seat	38	39	40
14	Left side of Wheelchair	41	42	43
15	Left bottom of seat	44	45	46
16	Left Caster	47	48	49
17	Top back corner of Toilet seat.	50	51	52
18	Top front right corner of Toilet seat	53	54	55
19	Bottom front right corner of Toilet seat	56	57	58
20	Bottom back corner of Toilet seat	59	60	61
21	Top front right corner of the grab bar	62	63	64
22	Top bent right side of the grab bar	65	66	67
23	Bottom of grab bar above load cell	77	78	79

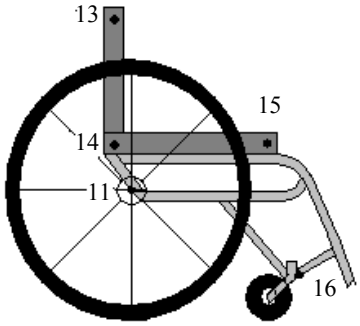

Diagram 1: wheelchair

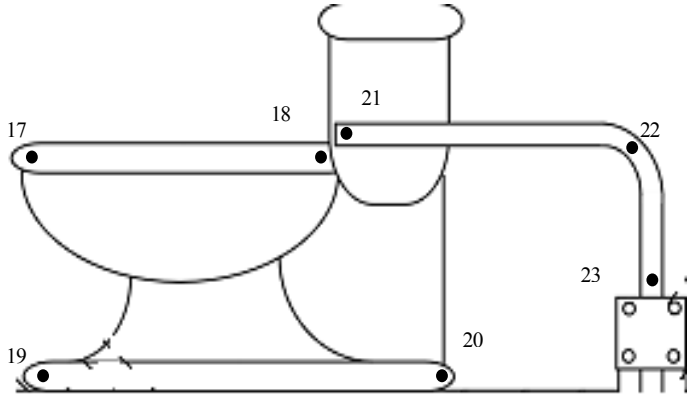

Diagram 2: Toilet

APPENDIX J

Set Position

In set position forearms were placed at a 90-degree angle forward from the upper arm, and the hand was aligned with the forearm with the fingers pointing straight forward, as shown in Figure 33.

Figure 33 Set position picture

APPENDIX K

```
subj_kin=input('Input newmofile: ','s');
eval(['load ' num2str(subj_kin)]);
eval(['kin =' num2str(subj_kin) ';'])
%side=input('Input the side of markers position(ex:R/L): ','s');

 rtmjx=kin(:,11);rtmjy=kin(:,12);rtmjz=-kin(:,13);
thirdmpx=kin(:,29);thirdmpy=kin(:,30);thirdmpz=-kin(:,31);
thirdmp=[thirdmpx,thirdmpy,thirdmpz];
radx=kin(:,26);rady=kin(:,27);radz=-kin(:,28);
rad=[radx,rady,radz];
ulnx=kin(:,23);ulny=kin(:,24);ulnz=-kin(:,25);
uln=[ulnx,ulny,ulnz];
olecx=kin(:,20);olecy=kin(:,21);olecz=-kin(:,22);
olec=[olecx,olecy,olecz];
latx=kin(:,17);laty=kin(:,18);latz=-kin(:,19);
lat=[latx,laty,latz];
acrox=kin(:,14);acroy=kin(:,15);acroz=-kin(:,16);
acro=[acrox,acroy,acroz];

 hubx=kin(:,32);huby=kin(:,33);hubz=-kin(:,34);
 kneex=kin(:,35); kneey=kin(:,36); kneez=-kin(:,37);
 backtopx=kin(:,38);backtopy=kin(:,39);backtopz=-kin(:,40);
 sbinsectx=kin(:,41);sbinsecty=kin(:,42);sbinsectz=-kin(:,43);
 seatfrontx=kin(:,44);seatfronty=kin(:,45);seatfrontz=-kin(:,46);
 casterx=kin(:,47);castery=kin(:,48);casterz=-kin(:,49);
 tb1x=kin(:,50);tb1y=kin(:,51);tb1z=-kin(:,52);
 tb2x=kin(:,53);tb2y=kin(:,54);tb2z=-kin(:,55);
 tb3x=kin(:,56);tb3y=kin(:,57);tb3z=-kin(:,58);
 tb4x=kin(:,59);tb4y=kin(:,60);tb4z=-kin(:,61);


 sternox=kin(:,2);sternoy=kin(:,3);sternoz=-kin(:,4);
 sterno=[sternox,sternoy,sternoz];
 c7x=kin(:,5);c7y=kin(:,6);c7z=-kin(:,7);
 c7=[c7x,c7y,c7z];
 t3x=kin(:,8);t3y=kin(:,9);t3z=-kin(:,10);
 t3=[t3x,t3y,t3z];
%view3d(thirdmp,fifthmp,rad,uln,olec,lat,acro,hub,chest1,chest2,chest3,subj_name,speed
,side)

figure(1)
set(1, 'Position', [20 20 900 700]);
clf

%if side=='r' | side=='l'
```

```
hold on

for i=1:length(kin)
  hold on
  %axis([0 0 -1500 1000 2000 1000]);
  %axis(axis);
  %grid on;
  %plot all lines
  plot([thirdmpy(i) rady(i)],[thirdmpz(i) radz(i)]),
   plot([thirdmpy(i) ulny(i)],[thirdmpz(i) ulnz(i)]),
   plot([ulny(i) olecy(i)],[ulnz(i) olecz(i)]),
   plot([olecy(i) laty(i)],[olecz(i) latz(i)]),
   plot([ulny(i) rady(i)],[ulnz(i) radz(i)]),
   plot([rady(i) laty(i)],[radz(i) latz(i)]),
   plot([acroy(i) laty(i)],[acroz(i) latz(i)]),
   plot([acroy(i) olecy(i)],[acroz(i) olecz(i)]),
   plot([c7y(i) t3y(i)],[c7z(i) t3z(i)]),

   %wheelchair
   plot([backtopy(i) sbinsecty(i)],[backtopz(i) sbinsectz(i)]),
   plot([sbinsecty(i) seatfronty(i)],[sbinsectz(i) seatfrontz(i)]),
   plot([seatfronty(i) castery(i)],[seatfrontz(i) casterz(i)]),

   %transfer bench
    plot([tb1y(i) tb2y(i)],[tb1z(i) tb2z(i)]),
    plot([tb1y(i) tb4y(i)],[tb1z(i) tb4z(i)]),
    plot([tb1y(i) tb3y(i)],[tb1z(i) tb3z(i)]),

  %plot all markers
  plot(thirdmpy(i),thirdmpz(i),'ko'),
  plot(rady(i),radz(i),'o'),
  plot(ulny(i),ulnz(i),'ko'),
  plot(laty(i),latz(i),'ko'),
  plot(olecy(i),olecz(i),'o'),
   plot(acroy(i),acroz(i),'o'),
   plot(huby(i),hubz(i),'o'),
   plot(kneey(i),kneez(i),'co'),
   plot(c7y(i),c7z(i),'ro'),
   plot(t3y(i),t3z(i),'ro'),
   plot(sternoy(i),sternoz(i),'ro'),
   %if side=='r'
      plot(rtmjy(i),rtmjz(i),'go'),
      plottitle=['sagittal plane plot for: ',subj_kin];
      TITLE(plottitle)
```

APPENDIX L

Car Seat Transfer

1. Sit in set position (**APPENDIX J**) for 2 seconds.
2. Place left hand on grab-bar target point, right hand on right wheel of wheelchair (a).
3. Transfer to edge of car seat by placing bottom on first target.
4. Shift to second target by placing left hand at the back corner of the car seat (b).
5. Move legs from wheelchair footrests to left mounting plate.
6. Return to the set position and stay in set position until the 20th second (c).
7. Place right hand at right back corner of the car seat, left hand on the grab-bar target point, and move back to edge of the car seat (first target) (d).
8. Place right hand on right wheel of the wheelchair, keeping left hand on grab-bar, and transfer back to wheelchair by moving the bottom (e).
9. Move legs from left mounting plate to footrest of wheelchair.
10. Return to set position and stay in set position till 40th second (f).

(a)

(b)

(c)

(d)

(e)

(f)

Figure 34 Car Seat Transfer

APPENDIX M

Tub Bench Transfer using Trapeze

1. Sit in set position (**APPENDIX J**) for 2 seconds.
2. Place left hand on far target of tub bench, right hand on trapeze (a).
3. Move legs towards left force-plate.
4. Transfer to tub bench, placing bottom on middle target (b).
5. Return to set position and stay in the set position until the 10th second(c).
6. Place left hand on trapeze, right hand on middle of wheelchair seat (d).
7. Move legs back towards right force-plate.
8. Transfer back to wheelchair, sliding right hand out from under bottom as necessary (e).
9. Return to set position for the duration of the trial (20 seconds)(f).

(a)

(b)

(c)

(d)

(e)

(f)

Figure 35 Tub bench transfer using trapeze

APPENDIX N

Tub Bench Transfer

1. Sit in set position (**APPENDIX J**) for 2 seconds.
2. Place left hand on middle target of tub bench, right hand on right front corner of wheelchair seat (a).
3. Move legs towards left force-plate.
4. Transfer to near target on tub bench (b).
5. Place left hand on far target of tub bench, right hand next to bottom on near target.
6. Shift bottom to middle target.
7. Return to set position and stay until the 10th second (c).
8. Place right hand on near target on tub bench and scoot bottom to near target.
9. Move legs back towards right force-plate.
10. Place right hand in middle of wheelchair seat, left hand on middle target (d).
11. Transfer back to wheelchair, sliding right hand out from under bottom as necessary (e).
12. Return to set position for the duration of the trial (20 seconds) (f).

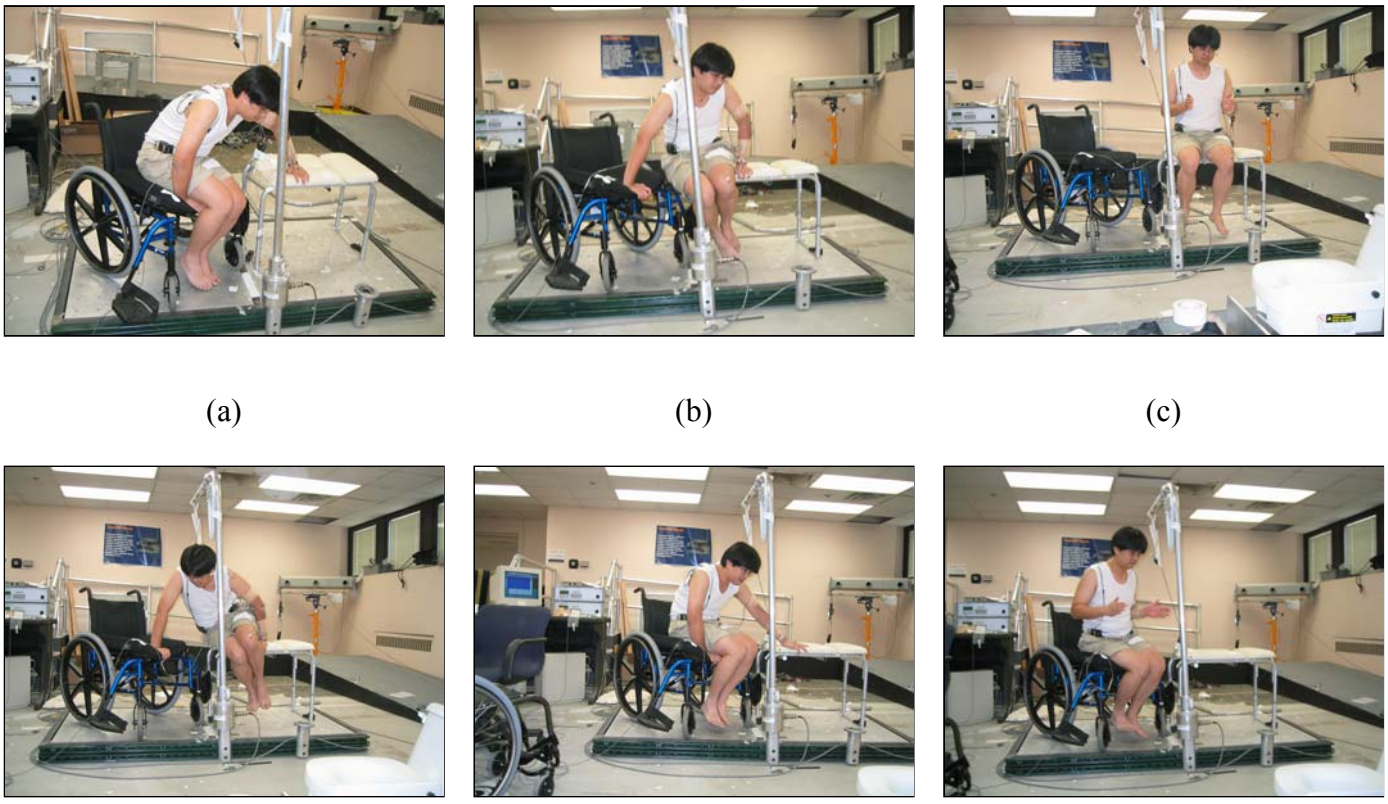

(a) (b) (c)

(d) (e) (f)

Figure 36 Tub bench transfer without using trapeze

APPENDIX O

Toilet Seat Transfer

1. Sit in set position (**APPENDIX J**) for 2 seconds.
2. Move bottom to front left corner of wheelchair seat.
3. Move legs towards left force-plate.
4. Place left hand on grab-bar target, right hand on front center of wheelchair seat(a).
5. Transfer to toilet seat(b).
6. Return to set position and stay until the 10th second(c).
7. Place left hand on grab-bar target, right hand on front center or center of wheelchair seat(d).
8. Move legs back towards right force-plate.
9. Transfer back to wheelchair, sliding right hand out from under bottom as necessary(e).
10. Return to set position for the duration of the trial (20 seconds)(f).

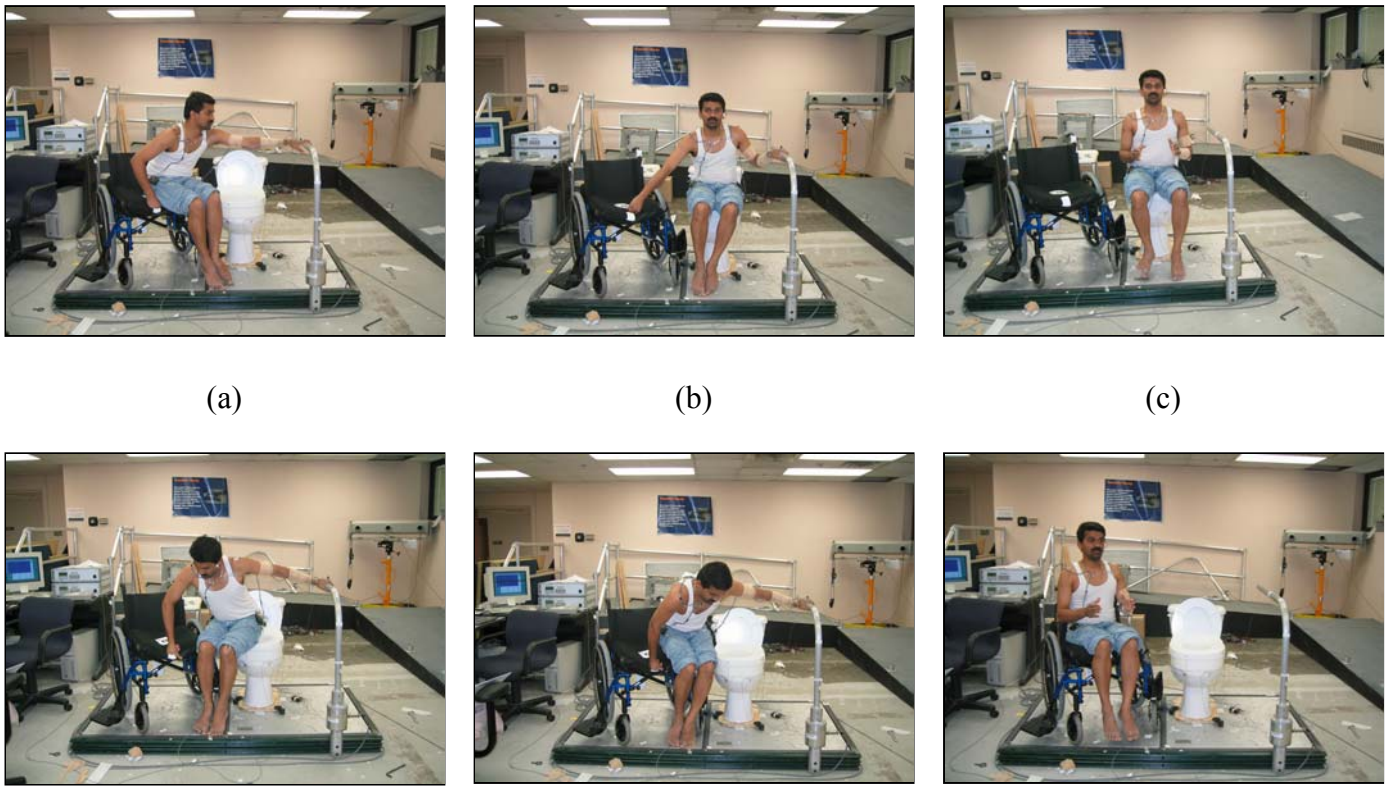

(a) (b) (c)

(d) (e) (f)

Figure 37 Toilet Seat Transfer

APPENDIX P

TwoPeakloadcell.m

```
% Calculate the two peaks loads during transfer from wheelchair to target surfaces and back
% using load cell data.
function [ans] = TwoPeakForce( file_string, int1_s, int1_e, int2_s, int2_e )

input = load(file_string);

f1x = max( abs( input(int1_s:int1_e,1) ) );
f1y = max( abs( input(int1_s:int1_e,2) ) );
f1z = max( abs( input(int1_s:int1_e,3) ) );


f2x = max( abs( input(int2_s:int2_e,1) ) );
f2y = max( abs( input(int2_s:int2_e,2) ) );
f2z = max( abs( input(int2_s:int2_e,3) ) );

ans = [f1x, f1y, f1z, f2x, f2y, f2z ];
return
```

APPENDIX Q

Interpolation.m

```
function [kin]=Interp_Clean(kin)

%This function replaces points dropped out in the
%kinematic files with interpolated points

size(kin)
[r,c]=size(kin);


for k=1:c;

n=1;
for i=1:2
if (kin(i,k)< -2*10e10);
if( i+n > r )
break;
end;
kin(i,k)=kin(i+n,k);
while kin(i+n,k)< -2*10e10
if( i+(n+1) > r )
break;
end;
kin(i+n,k)=kin(i+(n+1),k);
kin(i,k)=kin(i+n,k);
n=n+1;

end;
end;
for d=2:(n-1)
kin(d,k)=kin(i,k);
end;
end;

m=1;
for i=(r-1):r
if kin(i,k)< -2*10e10;
kin(i,k)=kin(i-m,k);
while kin(i-m,k)< -2*10e10
kin(i-m,k)=kin(i-(m+1),k);
kin(i,k)=kin(i-m,k);
m=m+1;
if( i-m > r )
break;
end;
```

```
end;
end;
for e=(r-(m+1)):(r-1)
kin(e,k)=kin(i,k);
end;
end;

for j=n:r-m;

if (kin(j,k)< -2*10e5)
dt=1200;
prev_pnt=kin(j-1,k);
next_pnt=kin(j+1,k);
cnt1=2;
while (next_pnt< -2*10e5)
next_pnt=kin(j+cnt1,k);
cnt1=cnt1+1;
end;
prev_pnt_2=kin(j-2,k);
next_pnt_2=kin((j+cnt1),k);
while (next_pnt_2< -2*10e5)
next_pnt_2=kin(j+(cnt1+1),k);
cnt1=cnt1+1;
end;
prev_slope=(prev_pnt-prev_pnt_2)/dt;
next_slope=(next_pnt_2-next_pnt)/dt;
temp_slope=abs((next_slope-prev_slope))/(cnt1+1);
a=2;
cnt2=cnt1-a;
c=0;
if (prev_slope>0) & (next_slope>0)
for b=1:(cnt1)
kin(j+c,k)=((prev_pnt+next_pnt)-cnt2)/2;
c=c+1;
cnt2=cnt2-2;
end;
elseif (prev_slope<0) & (next_slope<0)
for b=1:(cnt1)
kin(j+c,k)=((prev_pnt+next_pnt)+cnt2)/2;
c=c+1;
cnt2=cnt2-2;
end;
elseif (prev_slope>0) & (next_slope<0)
for b=1:(cnt1)
kin(j+c,k)=kin(j+(c-1),k)+(prev_slope-temp_slope)*dt;
prev_slope=(kin(j+c,k)-kin(j+(c-1),k))/dt;
```

```
c=c+1;
end;
elseif (prev_slope<0) & (next_slope>0)
for b=1:(cnt1)
kin(j+c,k)=kin(j+(c-1),k)+(prev_slope+temp_slope)*dt;
prev_slope=(kin(j+c,k)-kin(j+(c-1),k))/dt;
c=c+1;
end;
elseif (next_slope==0) | (prev_slope==0)
for b=1:(cnt1)
kin(j+c,k)=((prev_pnt+next_pnt)-cnt2)/2;
c=c+1;
cnt2=cnt2-2;
end;
end;
end;
end;
```

APPENDIX R

Forceplate.m

```
%function fp_v_n(rwhl)
%this program loads in the force plate raw data files and converts the data
%to meaningful forces and moments based on the manufacturer provided calibration
matrix.


[file,file_path]=uigetfile('*.*', 'select a baseline file');
file_string=[file_path, file];
baseline = load(file_string);
%fp=eval(strtok(file, ' '));
%baseline=tdfread(file)

rwhl_file=uigetfile('*.*','select a data file');
force_pl=load(rwhl_file);


Sl=[400.0 400.0 900.0 200.0 200.0 100.0]; %sensitivity for the left force plate
Sr=[400.0 400.0 900.0 200.0 200.0 100.0]; %sensitivity for the right force plate


for i=1:12
for j=1:length(force_pl)
fp(j,i)=(force_pl(j,i)-baseline(j,i));% Making the data starts from zero
end;
end;

fpr=fp(:,1:6);
fpl=fp(:,7:12);

for i=1:6
fpr(:,i)=fpr(:,i)*Sr(i);
fpl(:,i)=fpl(:,i)*Sl(i);
end


[b,a]=butter(4,20/200);       %a 4th order butterworth digital filter is used to sample the
signal
                              %with a cutoff frequency of 20/200 Hz, where 200=half of
                            % forceplate  sampling rate

for i=1:6;
fpr(:,i)=filtfilt(b,a,fpr(:,i));
fpl(:,i)=filtfilt(b,a,fpl(:,i));
end;
```

```
Fxf=(fpr(:,1));
Fyf=(fpr(:,2));
Fzf=(fpr(:,3));
Mxf=(fpr(:,4));
Myf=(fpr(:,5));
Mzf=(fpr(:,6));
Fxf=(fpl(:,1));
Fyf=(fpl(:,2));
Fzf=(fpl(:,3));
Mxf=(fpl(:,4));
Myf=(fpl(:,5));
Mzf=(fpl(:,6));

save fpr fpr -ascii -tabs
save fpl fpl -ascii -tabs

end
```

APPENDIX S

JointForcesMoments.m

```
% This program calculates the joint forces and moments at wrist, elbow and shoulder
using serial linkage mechanism concepts.

% Main function
function [result] = JointFM( file_string, Mass, height, len_ua, len_fa, w_t1, w_t2, t_w1,
t_w2 )
EPSILON = 0.000001;

% percentage of body weight coming at the hand during two transfers
forward_transfer_BW_percentage = 0.5484;
backward_transfer_BW_percentage = 0.7884;

kin=load(file_string);

% Lenth of input
len = length(kin);

% Get marker positions
sternox=kin(:,2);sternoy=kin(:,3);sternoz=kin(:,4);
sterno=[sternox,sternoy,sternoz]/1000.0;
c7x=kin(:,5);c7y=kin(:,6);c7z=kin(:,7);
c7=[c7x,c7y,c7z]/1000.0;
t3x=kin(:,8);t3y=kin(:,9);t3z=kin(:,10);
t3=[t3x,t3y,t3z]/1000.0;
tmjx=kin(:,11);tmjy=kin(:,12);tmjz=kin(:,13);
tmj=[tmjx,tmjy,tmjz]/1000.0;
acrox=kin(:,14);acroy=kin(:,15);acroz=kin(:,16);
acro=[acrox,acroy,acroz]/1000.0;
latx=kin(:,17);laty=kin(:,18);latz=kin(:,19);
lat=[latx,laty,latz]/1000.0;
olecx=kin(:,20);olecy=kin(:,21);olecz=kin(:,22);
olec=[olecx,olecy,olecz]/1000.0;
ulnx=kin(:,23);ulny=kin(:,24);ulnz=kin(:,25);
uln=[ulnx,ulny,ulnz]/1000.0;
radx=kin(:,26);rady=kin(:,27);radz=kin(:,28);
rad=[radx,rady,radz]/1000.0;
thirdmpx=kin(:,29);thirdmpy=kin(:,30);thirdmpz=kin(:,31);
thirdmp=[thirdmpx,thirdmpy,thirdmpz]/1000.0;


% Individual Mass  Calculated using  Winter's Method
mass_ua=0.028*(Mass);
mass_fa=0.016*(Mass);
mass_hand=0.006*(Mass);
```

```
% time interval between two consecutive data
time_factor = 1/120;

% Linear Velocity and Accelaration of marker points
vel_thirdmp = diff(thirdmp);
acc_thirdmp = diff(thirdmp,2);
vel_rad = diff(rad);
acc_rad = diff(rad,2);
vel_olec = diff(olec);
acc_olec = diff(olec,2);
vel_acro = diff(acro);
acc_acro = diff(acro,2);
vel_thirdmp = vel_thirdmp / time_factor;
acc_thirdmp = acc_thirdmp / time_factor^2;
vel_rad = vel_rad / time_factor;
acc_rad = acc_rad / time_factor^2;
vel_olec = vel_olec / time_factor;
acc_olec = acc_olec / time_factor^2;
vel_acro = vel_acro / time_factor;
acc_acro = acc_acro / time_factor^2;


% Angular velocity of arm segments
rel_pos_hand = thirdmp - rad;
rel_vel_hand = vel_thirdmp - vel_rad;

for i = 1: len-1
  %len_hand = sqrt( sum(rel_pos_hand(i,:).^2 ));
  ang_vel_hand(i,:) = cross( rel_pos_hand(i,:), rel_vel_hand(i,:)) /
sum(rel_pos_hand(i,:).^2 );
end

rel_pos_fa =  rad - olec;
rel_vel_fa =  vel_rad - vel_olec;
for i = 1: len-1
  ang_vel_fa(i,:) =  cross(rel_pos_fa(i,:), rel_vel_fa(i,:)) / (len_fa.^2);
end

rel_pos_ua = olec - acro;
rel_vel_ua = vel_olec - vel_acro;
for i=1: len-1
   ang_vel_ua(i,:) =  cross(rel_pos_ua(i,:), rel_vel_ua(i,:)) / (len_ua.^2);
end

ang_acc_hand = diff(ang_vel_hand);
ang_acc_fa = diff(ang_vel_fa);
```

```
ang_acc_ua =  diff(ang_vel_ua);

ang_acc_hand = ang_acc_hand / time_factor;
ang_acc_fa = ang_acc_fa / time_factor;
ang_acc_ua = ang_acc_ua / time_factor;


% MOI of arm segments calculated using Winter's method
MOI_ua =  mass_ua * ( 0.322 * 0.322 );
MOI_fa =  mass_fa * ( 0.303 * 0.303 );
MOI_hand = mass_hand * ( 0.297 * 0.297 );

% COG of arm segments calculated using Winter's method
% upperarm
uacg=0.564*acro+0.436*olec;
% forerarm
facg=0.57*olec+0.43*rad;
% hand
handcg = 0.494 * rad + 0.506 * thirdmp;


% Velocity, Accelaration of CG
vel_handcg = diff(handcg);
acc_handcg = diff(handcg,2);
vel_uacg = diff(uacg);
acc_uacg = diff(uacg,2);
vel_facg = diff(facg);
acc_facg = diff(facg,2);
vel_handcg = vel_handcg / time_factor;
acc_handcg = acc_handcg / time_factor^2;
vel_uacg = vel_uacg / time_factor;
acc_uacg = acc_uacg / time_factor^2;
vel_facg = vel_facg / time_factor;
acc_facg = acc_facg / time_factor^2;


% Inertia Force of CG
F_uacg   = -acc_uacg * mass_ua;
F_facg   = -acc_facg * mass_fa;
F_handcg = -acc_handcg * mass_hand;

% Inertia Moment about CG
M_uacg   = -ang_acc_ua * MOI_ua;
M_facg   = -ang_acc_fa * MOI_fa;
M_handcg = -ang_acc_hand * MOI_hand;
```

```
% Joint forces and moments using Free Body Diagram
% Force diagram for each segment and moment about centroid of each segment is used
% Groud direction is positive y-axis
ground = [ 0.0, 1.0, 0.0 ];

% external force  is calculated based on 54.84% of body weight during wh to tub bench
transfer
F_external = (Mass * 9.81 * forward_transfer_BW_percentage) * -ground;

for i= w_t1:w_t2
% Wrist
   F_wrist(i,:) = - [ (mass_hand * 9.81 * ground) + F_handcg(i,:) + F_external ];
   F_wrist_mag(i,:) = sqrt( sum(F_wrist(i,:).^2));
   M_wrist(i,:) = - [ M_handcg(i,:) +  cross((rad(i,:) - handcg(i,:)), F_wrist(i,:))  +
cross((thirdmp(i,:) - handcg(i,:)), F_external) ];
   M_wrist_mag(i,:) = sqrt( sum(M_wrist(i,:).^2));

% Elbow
   F_elbow(i,:) = - [ ( mass_fa * 9.81 * ground ) + F_facg(i,:) - F_wrist(i,:) ];
   F_elbow_mag(i,:) = sqrt( sum(F_elbow(i,:).^2));
   M_elbow(i,:) = - [ M_facg(i,:) + cross((rad(i,:) - facg(i,:)), -F_wrist(i,:)) +
cross((olec(i,:) - facg(i,:)), F_elbow(i,:)) ];
   M_elbow_mag(i,:) = sqrt( sum(M_elbow(i,:).^2));

% Shoulder
   F_shoulder(i,:) = - [ ( mass_ua * 9.81 * ground ) + F_uacg(i,:) - F_elbow(i,:) ];
   F_shoulder_mag(i,:) = sqrt( sum(F_shoulder(i,:).^2));
   M_shoulder(i,:) = - [ M_uacg(i,:) + cross((olec(i,:) - uacg(i,:)), -F_elbow(i,:)) +
cross((acro(i,:) - uacg(i,:)), F_shoulder(i,:)) ];
   M_shoulder_mag(i,:) = sqrt( sum(M_shoulder(i,:).^2));
end

% Peak inertia forces and moments
max_F_wrist_w_t = max( abs(F_wrist_mag) );
max_M_wrist_w_t = max( abs(M_wrist_mag) );

max_F_elbow_w_t = max( abs(F_elbow_mag) );
max_M_elbow_w_t = max( abs(M_elbow_mag) );

max_F_shoulder_w_t = max( abs(F_shoulder_mag) );
max_M_shoulder_w_t = max( abs(M_shoulder_mag) );
```

```
% external force  is calculated based on 78.84% of body weight during  tub bench to wh
transfer
F_external = (Mass * 9.81 * backward_transfer_BW_percentage) * -ground;

for i= t_w1:t_w2
% Wrist
   F_wrist(i,:) = - [ (mass_hand * 9.81 * ground) + F_handcg(i,:) + F_external ];
   F_wrist_mag(i,:) = sqrt( sum(F_wrist(i,:).^2));
   M_wrist(i,:) = - [ M_handcg(i,:) +  cross((rad(i,:) - handcg(i,:)), F_wrist(i,:))  +
cross((thirdmp(i,:) - handcg(i,:)), F_external) ];
   M_wrist_mag(i,:) = sqrt( sum(M_wrist(i,:).^2));

% Elbow
   F_elbow(i,:) = - [ ( mass_fa * 9.81 * ground ) + F_facg(i,:) - F_wrist(i,:) ];
   F_elbow_mag(i,:) = sqrt( sum(F_elbow(i,:).^2));
   M_elbow(i,:) = - [ -M_wrist(i,:) + M_facg(i,:) + cross((rad(i,:) - facg(i,:)), -F_wrist(i,:))
+ cross((olec(i,:) - facg(i,:)), F_elbow(i,:)) ];
   M_elbow_mag(i,:) = sqrt( sum(M_elbow(i,:).^2));

% Shoulder
   F_shoulder(i,:) = - [ ( mass_ua * 9.81 * ground ) + F_uacg(i,:) - F_elbow(i,:) ];
   F_shoulder_mag(i,:) = sqrt( sum(F_shoulder(i,:).^2));
   M_shoulder(i,:) = - [ -M_elbow(i,:) + M_uacg(i,:) + cross((olec(i,:) - uacg(i,:)), -
F_elbow(i,:)) + cross((acro(i,:) - uacg(i,:)), F_shoulder(i,:)) ];
   M_shoulder_mag(i,:) = sqrt( sum(M_shoulder(i,:).^2));
end

% Peak inertia forces and moments
max_F_wrist_t_w = max( abs(F_wrist_mag) );
max_M_wrist_t_w = max( abs(M_wrist_mag) );

max_F_elbow_t_w = max( abs(F_elbow_mag) );
max_M_elbow_t_w = max( abs(M_elbow_mag) );

max_F_shoulder_t_w = max( abs(F_shoulder_mag) );
max_M_shoulder_t_w = max( abs(M_shoulder_mag) );

result = [ max_F_wrist_w_t, max_M_wrist_w_t, max_F_elbow_w_t,
max_M_elbow_w_t, max_F_shoulder_w_t, max_M_shoulder_w_t,  max_F_wrist_t_w,
max_M_wrist_t_w, max_F_elbow_t_w, max_M_elbow_t_w, max_F_shoulder_t_w,
max_M_shoulder_t_w ]


return
```

BIBLIOGRAPHY

1. Nyland, J., Quigley, P., Huang, C., Lloyd, J., Harrow, J., and Nelson, A. Preserving Transfer Independence Among Individuals With Spinal Cord Injury. Spinal Cord 2000;38(11):649-57.

2. Somers MF, Spinal cord injury functional rehabilitation, 2nd Ed. 2 ed. Upper Saddle River, NJ: Prentice-Hall,Inc.; 2001.

3. Yarkony, G. M., Roth, E. J., Meyer, P. R., Jr., Lovell, L. L., and Heinemann, A. W. Rehabilitation Outcomes in Patients With Complete Thoracic Spinal Cord Injury. Am.J Phys.Med.Rehabil. 1990;69(1):23-7.

4. Yarkony, G. M., Roth, E. J., Heinemann, A. W., Lovell, L., and Wu, Y. C. Functional Skills After Spinal Cord Injury Rehabilitation: Three-Year Longitudinal Follow-Up. Arch.Phys.Med.Rehabil. 1988;69(2):111-4.

5. Subbarao, J. V., Klopfstein, J., and Turpin, R. Prevalence and Impact of Wrist and Shoulder Pain in Patients With Spinal Cord Injury. Journal of Spinal Cord Medicine 1994;18(1):9-13.

6. Allison, G. T., Singer, K. P., and Marshall, R. N. Transfer Movement Strategies of Individuals With Spinal Cord Injuries. Disabil.Rehabil. 1996;18(1):35-41.

7. Dalyan, M., Cardenas, D. D., and Gerard, B. Upper Extremity Pain After Spinal Cord Injury. Spinal Cord. 1999;37(3):191-5.

8. Nichols, P. J., Norman, P. A., and Ennis, J. R. Wheelchair User's Shoulder? Shoulder Pain in Patients With Spinal Cord Lesions. Scandinavian Journal of Rehabilitation Medicine 1979;11:29-32.

9. Pentland, W. E. and Twomey, L. T. The Weight-Bearing Upper Extremity in Women With Long Term Paraplegia. PARAPLEGIA 1991;29:521-30.

10. Sie, I. H., Waters, R. L., Adkins, R. H., and Gellman, H. Upper Extremity Pain in the Postrehabilitation Spinal Cord Injured Patient. Archives of Physical Medicine & Rehabilitation 1992;73:44-8.

11. Curtis, K. A., Roach, K. E., Applegate, E. B., Amar, T., Benbow, C. S., Genecco, T. D., and Gualano, J. Development of the Wheelchair User's Shoulder Pain Index (WUSPI). PARAPLEGIA 1995;33(5):290-3.

12. Calder, C. J. and Kirby, R. L. Fatal Wheelchair-Related Accidents in the United States. Am.J.Phys.Med.Rehabil. 1990;69(4):184-90.

13. Ummat, S. and Kirby, R. L. Nonfatal Wheelchair-Related Accidents Reported to the National Electronic Injury Surveillance System. American Journal of Physical Medicine & Rehabilitation 1994;73(3):163-7.

14. Allison, G. T. and Singer, K. P. Assisted Reach and Transfers in Individuals With Tetraplegia: Towards a Solution. Spinal Cord 1997;35:217-22.

15. Reyes, M. L., Gronley, J. K., Newsam, C. J., Mulroy, S. J., and Perry, J. Electromyographic Analysis of Shoulder Muscles of Men With Low-Level Paraplegia During a Weight Relief Raise. Archives of Physical Medicine and Rehabilitation 1995;76(5):433-9.

16. Perry, J., Gronley, J. K., Newsam, C. J., Reyes, M. L., and Mulroy, S. J. Electromyographic Analysis of the Shoulder Muscles During Depression Transfers in Subjects With Low-Level Paraplegia. Arch.Phys.Med.Rehabil. 1996;77(4):350-5.

17. Bayley, J. C., Cochran, T. P., and Sledge, C. B. The Weight-Bearing Shoulder. The Impingement Syndrome in Paraplegics. Journal of Bone & Joint Surgery - American Volume 1987;69:676-8.

18. Finley, M. A. and Rodgers, M. M. Prevalence and Identification of Shoulder Pathology in Athletic and Nonathletic Wheelchair Users With Shoulder Pain: A Pilot Study. Journal of Rehab R & D 2004;41:395-402.

19. Flatow EL, Soslowsky LJ, Ticker JB, Pawluk RJ, Hepler M, Ark J, Mow VC, and BiglianiLU. Excursion of the Rotator Cuff Under the Acromion. Patterns of Subacromial Contact. American Orthopaedic Society for Sports Medicine 1994;22(6):779-88.

20. Ludewig, P. M. and Cook, T. M. Alterations in Shoulder Kinematics and Associated Muscle Activity in People With Symptoms of Shoulder Impingement. Physical Therapy 2000;80(3):276-91.

21. Lukasiewicz, A. C., McClure, P., Michener, L., Pratt, N., and Sennett, B. Comparison of 3-Dimensional Scapular Position and Orientation Between Subjects With and Without Shoulder Impingement. J Orthop.Sports Phys.Ther. 1999;29(10):574-83.

22. Wang, Y. T., Kim, C. K., Ford, H. T. 3rd, and Ford, H. T., Jr. Reaction Force and EMG Analyses of Wheelchair Transfers. Perceptual & Motor Skills 1994;79(2):763-6.

23. Butler EE, Sabelman EE, and Kiratli BJ. Accelerometric Analysis of Wheelchair/Car Transfer Strategies for Individuals With Spinal Cord Injuries. Proceedings of the 2nd National Department of VA Rehabilitation R&D Conference, Washington, D.C, Feb.20-22, 2000 2000.

24. Invacare Fixed Offset Trapeze Bar. http://www.carepathways.com 3-29-2005.

25. Cooper, R. A., Boninger, M. L. Shimada S. D., and Lawrence, B. M. Glenohumeral Joint Kinematics and Kinetics for Three Coordinate System Representations During Wheelchair Propulsion. American Journal of Physical Medicine & Rehabilitation 1999;78(5):435-46.

26. Boninger, M. L., Cooper, R. A., Shimada, S. D., and Rudy, T. E. Shoulder and Elbow Motion During Two Speeds of Wheelchair Propulsion: a Description Using a Local Coordinate System. Spinal Cord 1998;36:418-26.

27. Boninger, M. L., Cooper, R. A., Robertson, R. N., and Rudy, T. E. Wrist Biomechanics During Two Speeds of Wheelchair Propulsion: an Analysis Using a Local Coordinate System. Archives of Physical Medicine & Rehabilitation 1997;78(4):364-72.

28. Yang Y, Koontz AM, Cooper RA, and Boninger ML. Trunk Movement Adaptations During Wheelchair Propulsion at Two Speeds and Load Conditions. Proceedings of the RESNA 2002 Annual Conference, Minneapolis, MN, June 28 - July 1 2002.

29. Spearman-Brown Prediction Formula. http://encyclopedia.lockergnome.com/s/b/Spearman-Brown_prediction_formula 4-17-2005.

30. Shigley J.E, Kinematic Analysis of Mechanisms. 2nd ed.Mcgraw-Hill College; 6-1-1969.

31. George H.Martin, Kinematics and Dynamics of Machines. 2nd ed.Waveland Pr Inc; 2002.

32. Winter, D. A., Biomechanics and Motor Control of Human Movement. 2 ed. New York: John Wiley & Sons; 1990.

33. Steven C.Chapra and Raymond Canale, Numerical Methods for Engineers: With Software and Programming Applications. 4 ed.McGraw-Hill Science/Engineering/Math; 7-16-2001.

34. John Joseph Uicker, Gordon R.Pennock, Joseph E.Shigley, John J., Jr. Uicke, and G.R.Pennock, Theory of Machines and MechanismsOxford University Press. Inc; 2003.

35. Finley, M. A., McQuade K.J., and Rodgers, M. M. Scapular Kinematics During Transfers in Manual Wheelchair Users With and Without Shoulder Impingement. Clinical Biomechanics 2005;20(1):32-40.

36. Megan Yarnall, Alicia M.Koontz, Yusheng Yang, Robert Price, and Michael L.Boninger. Wrist Range of Motion During Lateral Transfers Among Persons With Paraplegia. RESNA Proceeding 2005.

37. Harvey, L. A. and Crosbie, J. Biomechanical Analysis of a Weight-Relief Maneuver in C5 and C6 Quadriplegia. Arch.Phys.Med.Rehabil 2000;81(4):500-5.